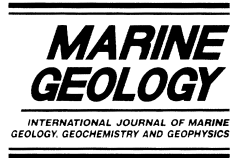




ELSEVIER

Marine Geology 156 (1999) 159–186



## Benthic foraminiferal paleoceanography of the South China Sea over the last 40,000 years

Zhimin Jian <sup>a,\*</sup>, Luejiang Wang <sup>c</sup>, Markus Kienast <sup>b</sup>, Michael Sarnthein <sup>c</sup>, Wolfgang Kuhnt <sup>c</sup>,  
Huiling Lin <sup>d</sup>, Pinxian Wang <sup>a</sup>

<sup>a</sup> Laboratory of Marine Geology, Tongji University, Shanghai 200092, China

<sup>b</sup> Department of Earth and Ocean Sciences, University of British Columbia, Vancouver, BC V6T 1Z4, Canada

<sup>c</sup> Institute of Geology and Paleontology, Kiel University, Kiel 24118, Germany

<sup>d</sup> Institute of Marine Geology, Sun Yat-Sen University, Kaohsiung, Taiwan 804, China

Received 18 February 1997; accepted 20 May 1998

---

### Abstract

Benthic foraminifera in gravity and piston cores from two sites of the northern and southern slopes of the South China Sea (SCS) were analyzed to evaluate changes in surface productivity and deep-water mass characteristics over the last 40,000 years. Our observations suggest that changes in organic carbon flux, that is food supply, and chemical and/or physical properties of the ambient water mass may be the two primary and intercorrelated factors controlling the distribution patterns of benthic foraminifera. When organic carbon flux increased above  $3.5 \text{ g C m}^{-2} \text{ yr}^{-1}$  in the southern SCS during the last glacial maximum and in the northern SCS during the first part of the Holocene around 10 ka B.P., a group of detritus feeders including *Bulimina aculeata* and *Uvigerina peregrina* dominated the benthic foraminiferal assemblage as shown by relative abundance (%) and accumulation rates. This may reflect episodes of increased surface productivity, possibly induced by increased input of nutrients from nearby river runoff. Suspension feeders such as *Cibicidoides wuellerstorfi* and a group of ‘opportunistic’ species including *Oridorsalis umbonatus*, *Melonis barleeanum* and *Chilostomella ovoidea* gradually became more abundant than detritus feeders as soon as the organic carbon flux decreased to  $2.5\text{--}3.5 \text{ g C m}^{-2} \text{ yr}^{-1}$ . Similar glacial to interglacial changes in relative abundance and accumulation rates were observed in both cores for a number of species, including *Eggerella bradyi*, *Globocassidulina subglobosa*, *Astrononion novozealandicum*, *Sphaeroidina bulloides* and *Cibicidoides robertsonianus*. These changes were not correlated to the distribution patterns of organic carbon in both cores and may have been related to yet unspecified changes in chemical and/or physical properties of the ambient water mass, independent of changes in organic carbon flux. © 1999 Elsevier Science B.V. All rights reserved.

**Keywords:** benthic foraminifera; organic carbon flux; water mass properties; East Asian monsoon; South China Sea

---

\* Corresponding author. Fax: +86-21-6513-8808; E-mail: zjiank@online.sh.cn

## 1. Introduction

Over the last 20 years deep-sea benthic foraminifera were extensively used to monitor climatically driven changes in deep-water conditions during the late Quaternary (e.g. Corliss et al., 1986; Boyle, 1990). Many investigators searched for causal links between the spatial and temporal variations of deep-sea benthic foraminiferal communities and various properties of deep-water masses (Streeter, 1973; Lohmann, 1978; Streeter and Shackleton, 1979; Douglas and Woodruff, 1981; Hermelin and Shimmield, 1990; Jian and Wang, 1997). Other investigators, however, claimed that abundance and species composition of benthic foraminiferal fauna were closely linked to the flux of organic carbon to the seafloor and, hence, to seasonal surface productivity (Altenbach, 1988; Herguera, 1992; Corliss, 1994; Sarnthein and Altenbach, 1995; Thomas et al., 1995; Miao and Thunell, 1996; Kuhnt et al., 1999). Therefore, the relationship between variation patterns of benthic foraminifera and surface productivity, organic carbon flux, and deep-water masses has been a point of vigorous discussion in recent years.

The modern distribution of deep-sea benthic foraminifera is of special interest to understand this relationship. However, this type of study has not been carried out in the South China Sea (SCS) until the last few years (Jian and Zheng, 1992; Miao and Thunell, 1993, 1996; Jian and Wang, 1997; Kuhnt et al., 1999). Earlier works (Tu, 1983; Zheng, 1987) concentrated on taxonomic inventories of the SCS. Based on the very close correlation of modern benthic foraminiferal assemblages to water depth in the SCS, Miao and Thunell (1993, 1996) and Kuhnt et al. (1999) argued that changes in organic carbon flux to the seafloor could be the most important controlling factor. By contrast, Jian and Wang (1997) emphasized that fluctuations in assemblage composition reflected general trends of late Quaternary variations in deep-water masses, especially in oligotrophic regions. In addition, species-specific microhabitat preferences (Corliss, 1985; Rathburn and Corliss, 1994) and taphonomic problems (Loubere and Gray, 1990; Kuhnt et al., 1999) complicated the interpretation of glacial–interglacial changes based on benthic foraminiferal assemblages.

As a marginal sea, the SCS has sedimentation rates higher by an order of magnitude than the Pacific, and its widespread carbonate sediments provide an ideal basis for high-resolution paleoceanographic reconstruction. During the last glacial maximum the SCS changed into a semi-enclosed basin with the Bashi Strait being the only deep-water gateway to the open western Pacific Ocean (Wang, 1990; Wang and Wang, 1990). This led to a pronounced difference in deep-water circulation which, coupled with a high-resolution stratigraphic record, offers a unique opportunity to understand glacial–interglacial changes in deep-water environments (Jian and Wang, 1997).

The SCS witnessed dramatic changes in productivity, hydrography, and depositional environments during the late Quaternary glacial cycles (Wang, 1990; Wang and Wang, 1990; Thunell et al., 1992; Schönfeld and Kudrass, 1993; Miao et al., 1994; P. Wang et al., 1995). These changes would have altered, directly and indirectly, the benthic environment. In this study, we examine high-resolution variations in deep-sea benthic foraminifera, stable isotopes, and organic carbon flux from gravity and piston cores at two sites in the SCS. We use this information to evaluate changes in deep-water conditions in the SCS over the last 40,000 years, and to improve our understanding of climate change in Southeast Asia and of the hydrological and carbon cycles in the SCS during the last glacial and the Holocene.

## 2. Material

We studied one piston and two gravity cores (Fig. 1; Table 1) raised from the southern and northern slopes of the SCS during the *Sonne-95* cruise in 1994 (Sarnthein et al., 1994). The sediment in the cores consists of dark-gray silty clay which shows no evidence of turbiditic or mass flow deposition nor of major reworking. All cores were sampled at 5–20 cm intervals, isotope analyses were carried out for the whole set of samples (>300) and a total of 169 samples were analyzed for benthic foraminiferal studies (Table 2). According to the AMS  $^{14}\text{C}$  age data and oxygen isotopic stratigraphy (Wang et al., 1999), our samples have a high temporal resolution between 81 and 1346 years (Table 1).

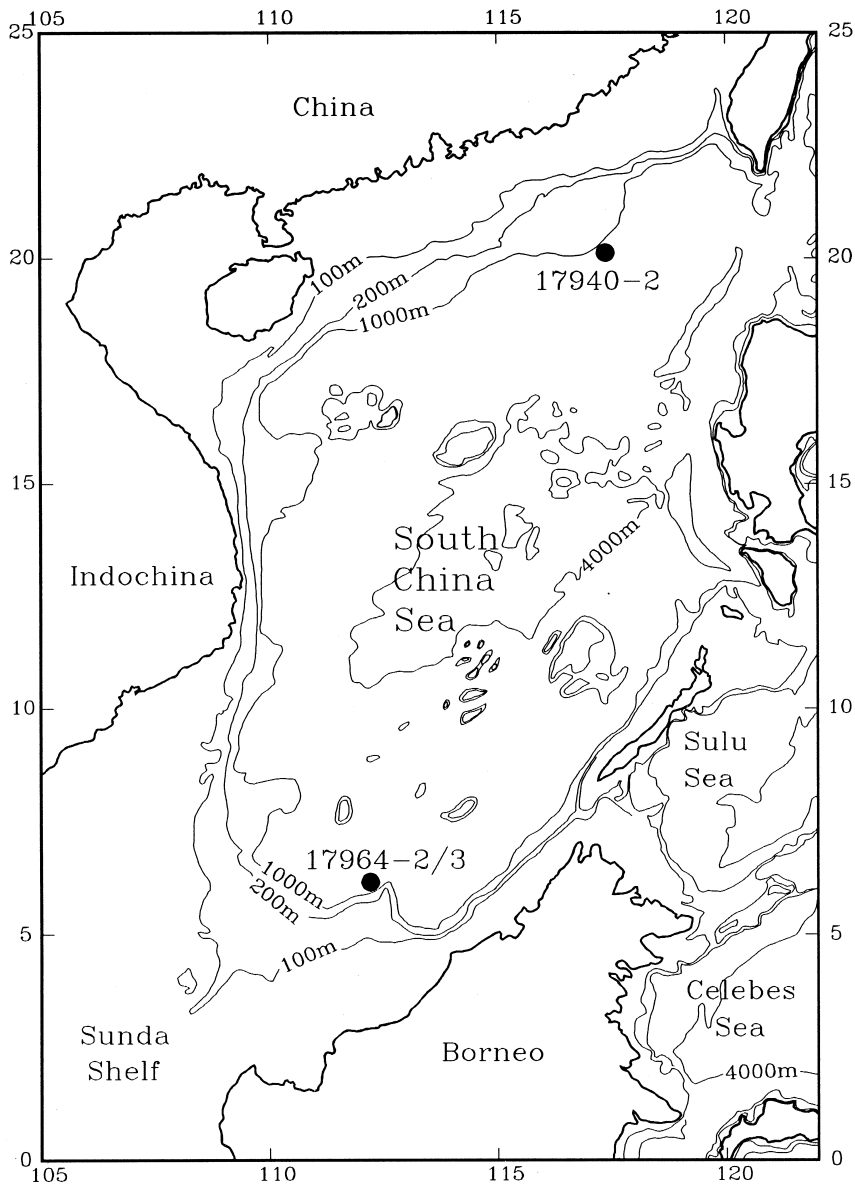


Fig. 1. Location of the South China Sea cores used in this study.

Table 1

Location, water depth and sample information of the cores used in this study

| Core                 | Type    | Latitude (N) | Longitude (E) | Water depth (m) | Core length (cm) | Nr. of samples | Sampling interval (cm) | Time resolution (yr) |
|----------------------|---------|--------------|---------------|-----------------|------------------|----------------|------------------------|----------------------|
| 17940-2              | gravity | 20°07.0'     | 117°23.0'     | 1727            | 1330             | 91             | 5–20                   | 81–1346              |
| 17964-2 <sup>a</sup> | piston  | 06°09.5'     | 112°12.8'     | 1556            | 1304             | 34             | 20                     | 261–372              |
| 17964-3              | gravity | 06°09.5'     | 112°12.8'     | 1556            | 912              | 44             | 20                     | 316–910              |

<sup>a</sup> Only the part below 600 cm was studied.

### 3. Methods

#### 3.1. Age control

Oxygen and carbon stable isotope measurements were carried out on the planktonic foraminiferal species *Globigerinoides ruber* (>315  $\mu\text{m}$ ) and benthic foraminiferal species *Cibicidoides wuellerstorfi* (>315  $\mu\text{m}$ ), using a Finnigan MAT 251 mass spectrometer at the University of Kiel (Wang et al., 1999).

AMS  $^{14}\text{C}$  ages of planktonic foraminiferal species *G. ruber* or *Globigerinoides sacculifer* in 20 samples of core 17940-2 and 6 samples of core 17964-3 were generated at the Leibniz-Laboratory of the Institut für Kernphysik, Kiel, to provide stratigraphic controls for the cores. The results of stable isotopes and AMS  $^{14}\text{C}$  datings are discussed in detail in a separate paper (Wang et al., 1999).

#### 3.2. Organic carbon and carbonate analyses

After drying an aliquot of the sediment and grinding to a fine power, the organic and inorganic carbon contents of 321 samples were measured using the CHN-Analyzer at the University of Kiel and a LECO carbon analyzer at the Sun Yat-Sen University in Kaohsiung. Then carbonate contents were calculated from the inorganic carbon contents. A more detailed description of organic carbon and carbonate analyses can be found in Wang et al. (1999).

To avoid a possible influence of dilution by terrigenous and other material, fluctuations of organic carbon (Corg) and carbonate are expressed by mass accumulation rates (MAR) with  $\text{MAR (g cm}^{-2} \text{ kyr}^{-1}) = \text{content (\%)} \times \text{sedimentation rate (cm kyr}^{-1}) \times \text{dry bulk density (g cm}^{-3})$  (Thunell et al., 1992; Schönfeld and Kudrass, 1993). In addi-

tion, based on the Corg content in the cores, Corg flux and export productivity were estimated using the equations of Sarnthein et al. (1992), to test the relationship between productivity and benthic foraminiferal distribution.

#### 3.3. Faunal studies

All samples were disintegrated in demineralized water and washed over a 63  $\mu\text{m}$  screen. The residues were sieved in fractions of 63–150  $\mu\text{m}$ , 150–250  $\mu\text{m}$ , 250–630  $\mu\text{m}$  and >630  $\mu\text{m}$ . Benthic foraminifera were picked and counted from the size fraction >150  $\mu\text{m}$ . When necessary, the sample was split using a standard Otto-microsplitter to yield a subsample containing at least 300 specimens. The average counted number of benthic foraminifera per sample is 214, 409 and 332 in cores 17940-2, 17964-2 and 17964-3, respectively (Table 2).

Benthic foraminifera were counted and identified using the taxonomic works of Barker (1960), Saidova (1975), Lutze (1980) and Ujiié (1990). In general, foraminifera were identified to the species or subspecies level. However, some unidentifiable agglutinated and porcellaneous forms were grouped together. *Milionella*, *Lagena*, *Fissurina*, *Oolina*, *Nodosaria*, *Dentalina*, *Guttulina*, *Lenticulina* and *Elphidium* were counted at genera level because of the high species diversity and low relative abundance of each species. Seventy-three genera including 112 species or subspecies were identified in this study (Table 2).

Based on the down-core census data (Appendixes A and B), the abundance of benthic foraminifera (individuals per gram sediment), the species diversity (given as Shannon–Weaver index values  $H(S)$ ), the relative ratios of porcellaneous and agglutinated benthic foraminifera, the percentage of

Table 2  
Information of foraminiferal faunal analysis in this study

| Core    | Number counted per sample |         |         | Genera (species) identified |
|---------|---------------------------|---------|---------|-----------------------------|
|         | minimum                   | maximum | average |                             |
| 17940-2 | 93                        | 430     | 214     | 68 (100)                    |
| 17964-2 | 212                       | 682     | 409     | 43 (63)                     |
| 17964-3 | 164                       | 746     | 332     | 59 (87)                     |

Table 3

The matrix of factor scores of the three Q-mode varimax factors in core 17940-2

| Species/species groups          | Factor 1 | Factor 2 | Factor 3 | Species/species groups               | Factor 1 | Factor 2 | Factor 3 |
|---------------------------------|----------|----------|----------|--------------------------------------|----------|----------|----------|
| <i>Siphotextularia flintii</i>  | 0.015    | 0.002    | 0.008    | <i>Globocassidulina subglobosa</i>   | 0.216    | -0.029   | 0.190    |
| <i>Texturalia</i> spp.          | 0.011    | 0.088    | -0.001   | <i>Chilostomella ovoidea</i>         | 0.024    | 0.732    | 0.036    |
| <i>Eggerella bradyi</i>         | 0.148    | 0.015    | 0.108    | <i>Pullenia bulloides</i>            | 0.079    | 0.018    | 0.024    |
| <i>Martinottiella communis</i>  | 0.113    | -0.008   | 0.104    | <i>Pullenia quinqueloba</i>          | 0.052    | 0.053    | 0.038    |
| <i>Pyrgo</i> spp.               | 0.011    | 0.076    | 0.019    | <i>Melonis barleeaanum</i>           | 0.019    | 0.263    | 0.109    |
| <i>Triloculina tricarinata</i>  | -0.011   | 0.073    | -0.009   | <i>Astrononion novozealandicum</i>   | 0.146    | -0.032   | 0.050    |
| <i>Quinqueloculina</i> spp.     | 0.000    | 0.050    | 0.009    | <i>Astrononion stellatus</i>         | -0.007   | 0.045    | 0.000    |
| <i>Cornuspira planorbis</i>     | 0.006    | 0.052    | -0.021   | <i>Ceratobulimina pacifica</i>       | 0.137    | -0.062   | 0.131    |
| Miliolids                       | 0.005    | 0.084    | -0.007   | <i>Epistominella exigua</i>          | 0.026    | -0.010   | 0.012    |
| <i>Lagena</i> spp.              | 0.034    | 0.123    | 0.089    | <i>Shpaeroidina bulloides</i>        | 0.160    | 0.160    | 0.053    |
| <i>Fissurina</i> spp.           | 0.079    | 0.174    | 0.119    | <i>Valvulineria glabra</i>           | 0.009    | 0.134    | 0.002    |
| <i>Nodosaria</i> spp.           | 0.002    | 0.046    | 0.025    | <i>Anomalina globulosa</i>           | 0.027    | 0.000    | 0.009    |
| <i>Dentalina</i> spp.           | 0.041    | 0.017    | 0.003    | <i>Hanzawaia concentrica</i>         | -0.037   | 0.154    | -0.028   |
| <i>Lenticulina</i> spp.         | 0.025    | 0.019    | 0.017    | <i>Gavelinopsis translucens</i>      | -0.018   | 0.093    | -0.003   |
| <i>Bolivinita quadrilatera</i>  | -0.021   | 0.060    | 0.006    | <i>Oridorsalis umbonatus</i>         | 0.024    | 0.058    | 0.006    |
| <i>Bolivina pacifica</i>        | 0.003    | 0.026    | 0.012    | <i>Gyroidina broeckiana</i>          | 0.102    | -0.062   | 0.097    |
| <i>Globobulimina</i> spp.       | -0.077   | 0.335    | 0.037    | <i>Gyroidina orbicularis</i>         | 0.000    | 0.024    | 0.012    |
| <i>Bulimina alazanensis</i>     | -0.008   | 0.027    | 0.008    | <i>Gyroidinoides lamarckiana</i>     | 0.026    | 0.004    | 0.032    |
| <i>Bulimina aculeata</i>        | 0.081    | -0.089   | 0.8180   | <i>Gyroidina nitida</i>              | -0.007   | 0.076    | 0.018    |
| <i>Bulimina mexicana</i>        | -0.001   | 0.126    | 0.068    | <i>Osangularia culter</i>            | 0.080    | -0.028   | 0.108    |
| <i>Uvigerina peregrina</i>      | 0.003    | 0.035    | 0.104    | <i>Epistominella rugosa</i>          | -0.018   | 0.083    | -0.005   |
| <i>Uvigerina auferiana</i>      | 0.874    | 0.030    | -0.290   | <i>Cibicidoides robertsonianus</i>   | 0.094    | 0.004    | 0.109    |
| <i>Rutherfordoides</i> sp.      | -0.036   | 0.132    | -0.002   | <i>Cibicidoides wuellerstorfi</i>    | -0.068   | 0.189    | 0.025    |
| <i>Cassidulina laevigata</i>    | 0.071    | -0.007   | 0.140    | <i>Cibicidoides pseudoungerianus</i> | 0.118    | -0.081   | 0.230    |
| <i>Globocassidulina elegans</i> | 0.023    | -0.009   | 0.005    | <i>Cibicides lobatulus</i>           | -0.017   | 0.068    | -0.014   |

presumed infaunal calcareous benthic foraminifera, and the percentage abundance of each species were calculated. The percentage data of the most abundant species were plotted against composite depth in core to illustrate the down-core distribution patterns.

Q-mode factor analysis was carried out on the faunal census data using the program of Klován and Imbrie (1971). Factor analysis is a multivariable statistical technique for reducing the number of variables, in this case benthic foraminiferal taxa, and thereby enabling easier determination of benthic foraminiferal assemblages. Only species with relative abundance exceeding 2% in at least two samples (50 species and species-groups in core 17940-2, see Table 3; and 38 in cores 17964-2 and 17964-3, see Table 4) were included in the factor analyses.

In order to exclude the dilution of benthic foraminifera with terrigenous or planktonic foraminiferal material, and to evaluate the effect of Corg and carbonate accumulation rates on the changes in benthic foraminiferal accumulation through time, the

accumulation rates of some species were determined using the following equation:

$$AR = (\text{Foram}) \cdot (\text{SR}) \cdot (\text{DBD})$$

where: AR is the accumulation rate ( $n \text{ cm}^{-2} \text{ kyr}^{-1}$ ); Foram is the abundance of foraminifera ( $n \text{ g}^{-1}$ ); SR is the sedimentation rate ( $\text{cm kyr}^{-1}$ ); and DBD is the dry bulk density of sediment ( $\text{g cm}^{-3}$ ).

Carbonate dissolution/preservation is evaluated using changes in planktonic foraminiferal fragmentation, benthic foraminiferal ratio to the total foraminiferal fauna, and relative abundance of the planktonic foraminifera *Pulleniatina obliquiloculata*. Planktonic foraminiferal fragmentation is expressed as:

$$\text{Fragmentation} = F/(F + W) \%$$

where: *F* is the number of planktonic foraminiferal fragments in the sample; and *W* is the total number of well-preserved planktonic foraminifera in the sample (Thunell, 1976; Miao and Thunell, 1996).

Table 4

The matrix of factor scores of the two Q-mode varimax factors in core 17964-2/3

| Species/species groups            | Factor 1 | Factor 2 | Species/species groups               | Factor 1 | Factor 2 |
|-----------------------------------|----------|----------|--------------------------------------|----------|----------|
| <i>Siphotextularia flintii</i>    | −0.006   | 0.053    | <i>Uvigerina auberiana</i>           | 0.002    | 0.050    |
| <i>Textularia</i> spp.            | −0.012   | 0.067    | <i>Cassidulina laevigata</i>         | −0.001   | 0.317    |
| <i>Eggerella bradyi</i>           | −0.052   | 0.356    | <i>Globocassidulina subglobosa</i>   | −0.029   | 0.132    |
| <i>Martinottiella communis</i>    | −0.044   | 0.194    | <i>Chilostomella ovoidea</i>         | −0.026   | 0.134    |
| <i>Sigmoilopsis schlumbergeri</i> | −0.009   | 0.113    | <i>Pullenia bulloides</i>            | −0.030   | 0.141    |
| Miscellaneous agglutinants        | −0.045   | 0.316    | <i>Pullenia quinqueloba</i>          | −0.011   | 0.082    |
| <i>Pyrgo</i> spp.                 | −0.011   | 0.139    | <i>Melonis barleeianum</i>           | −0.040   | 0.177    |
| <i>Pyrgoella sphaerica</i>        | 0.005    | 0.116    | <i>Astrononion novozealandicum</i>   | −0.047   | 0.189    |
| <i>Triloculina tricarinata</i>    | 0.000    | 0.046    | <i>Ceratobulimina pacifica</i>       | −0.033   | 0.144    |
| <i>Quinqueloculina</i> spp.       | 0.021    | 0.074    | <i>Epistominella exigua</i>          | −0.003   | 0.062    |
| Miliolids                         | 0.016    | 0.116    | <i>Sphaeroidina bulloides</i>        | −0.018   | 0.121    |
| <i>Lagena</i> spp.                | 0.001    | 0.107    | <i>Hoeglundina elegans</i>           | −0.004   | 0.073    |
| <i>Fissurina</i> spp.             | 0.023    | 0.201    | <i>Oridorsalis umbonatus</i>         | 0.007    | 0.158    |
| <i>Dentalina</i> spp.             | −0.015   | 0.076    | <i>Gyroidina broeckhiana</i>         | −0.013   | 0.063    |
| <i>Bolivina robusta</i>           | 0.038    | 0.006    | <i>Gyroidinoides lamarckiana</i>     | −0.018   | 0.089    |
| <i>Globobulimina affinis</i>      | 0.026    | 0.061    | <i>Osangularia culter</i>            | −0.027   | 0.135    |
| <i>Bulimina aculeata</i>          | 0.977    | 0.067    | <i>Cibicidoides robertsonianus</i>   | −0.050   | 0.326    |
| <i>Bulimina mexicana</i>          | −0.022   | 0.181    | <i>Cibicidoides wuellerstorfi</i>    | 0.009    | 0.278    |
| <i>Uvigerina peregrina</i>        | 0.147    | 0.192    | <i>Cibicidoides pseudoungerianus</i> | 0.006    | 0.103    |

## 4. Results

### 4.1. Stratigraphy and chronology

The stratigraphic controls are based on AMS  $^{14}\text{C}$  data for core 17940-2, and planktonic (*G. ruber*) and benthic (*C. wuellerstorfi*) foraminiferal oxygen isotopes as well as AMS  $^{14}\text{C}$  data for cores 17964-2 and 17964-3 (Wang et al., 1999). All the measured AMS  $^{14}\text{C}$  ages were converted to the calendar scale using the relationships between the  $^{14}\text{C}$  and the U/Th timescale found by Bard et al. (1990) (refer to Pearson et al., 1993; Stuiver and Becker, 1993; Stuiver and Braziunas, 1993; Wang et al., 1999). In Figs. 2–9 and 11–14 the calendar ages (lines with age numbers) are from Wang et al. (1999).

The gravity core 17964-3 and piston core 17964-2 at the same location (Table 1; Fig. 1) were carefully correlated. Their oxygen isotopic and carbonate curves can match each other if those of core 17964-2 are shifted 200 cm down-core (Wang et al., 1999). Therefore, in this study we used the corrected depth for core 17964-2, i.e. 0 cm in core 17964-2 equals to 200 cm in core 17964-3. For the benthic foraminiferal analysis, we studied only the part below 600 cm in core 17964-2 and appended it to core 17964-3 with a

short overlap of 68 cm. Thus, the composite core was called core 17964-2/3 in the following paragraphs.

The bases of cores 17940-2 and 17964-2/3 reach approximately 40 and 35 ka B.P., respectively. The sedimentation rate for core 17940-2 varied between 13.0 and 74.6 cm kyr $^{-1}$  with higher values during the Holocene, whereas that for core 17964-2/3 varied between 25.5 and 63.2 cm kyr $^{-1}$  with higher values during the last glacial, resulting in sample resolutions between 100 and 1000 years (Table 1).

### 4.2. Geochemical results

The Corg and carbonate contents in core 17940-2 varied between 0.70 and 1.26%, and 6.0 and 20.5%, respectively, while those in core 17964-2/3 varied between 0.71 and 0.95%, and 1.9 and 18.9%, respectively (Figs. 2 and 3). The Corg contents show no systematic or meaningful changes in both cores. However, the down-core fluctuations of carbonate contents in core 17964-2/3 display a glacial decrease and Holocene increase (Fig. 3), which has been attributed to increased glacial dilution by terrigenous material (Thunell et al., 1992; P. Wang et al., 1995). It should be noted that carbonate contents display an opposite trend in core 17940-2 (Fig. 3), which may

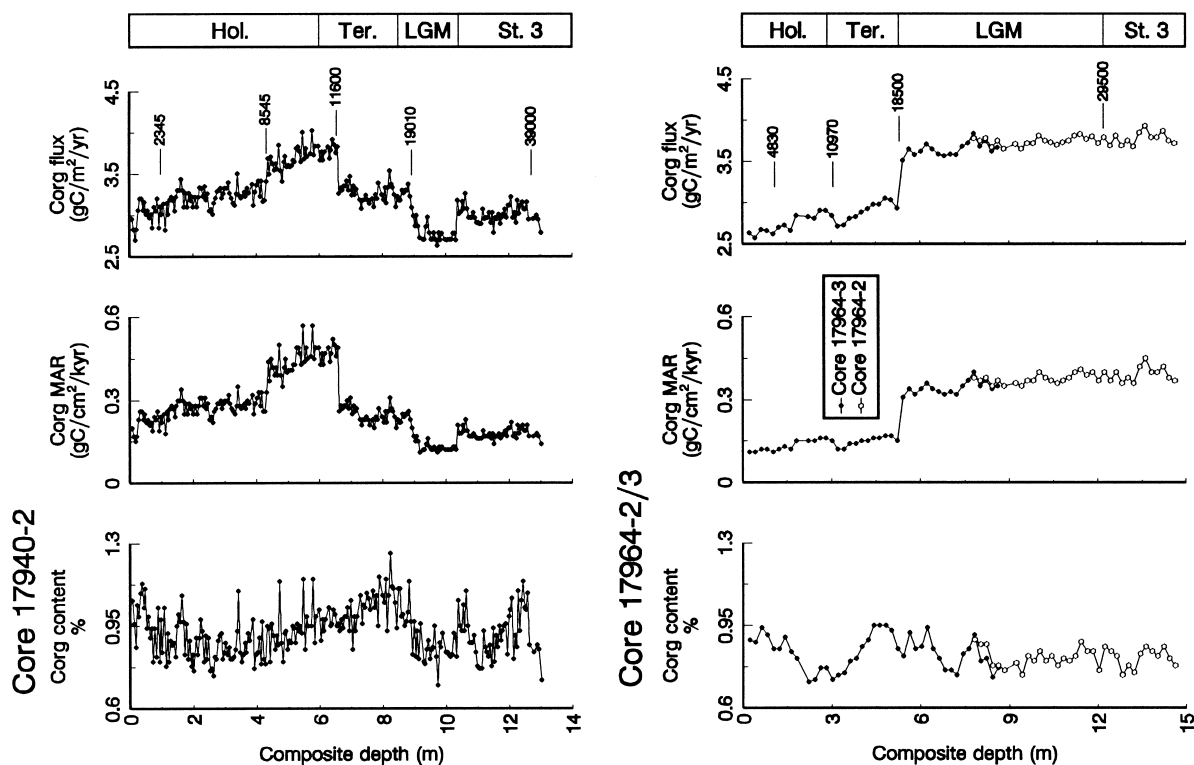


Fig. 2. Variations in Corg content (%), MAR ( $\text{g C cm}^{-2} \text{ kyr}^{-1}$ ) and flux ( $\text{g C m}^{-2} \text{ yr}^{-1}$ ) in cores 17940-2 and 17964-2/3. The added lines with calendar ages are from Wang et al. (1999). *Hol.*, *Ter.*, *LGM* and *St. 3* on the right side are abbreviated from Holocene, Termination I, last glacial maximum and  $\delta^{18}\text{O}$  stage 3, respectively.

be explained by higher terrigenous flux from Chinese rivers during the Holocene. The variations of  $\text{CaCO}_3$  MAR in cores 17940-2 and 17964-2/3 display a very similar pattern of glacial decrease and Holocene increase, with relatively higher values in core 17940-2 (1.8 to 8.8%) than in core 17964-2/3 (0.6 to 3.5%) (Fig. 3). The down-core variations in Corg MAR and Corg flux are more complicated (Fig. 2). The Corg flux is higher, with values of  $>3.5 \text{ g C m}^{-2} \text{ yr}^{-1}$  during the last glacial in core 17964-2/3 and during the early Holocene in core 17940-2, respectively (Fig. 2). These enhanced Corg fluxes may have been caused by increased surface productivity and/or enhanced input of terrigenous nutrients (Thunell et al., 1992; Winn et al., 1992).

#### 4.3. Benthic foraminiferal results

The absolute abundance of benthic foraminifera (number of specimens per gram) varied between

13.5 and 106.4, and between 14.5 and 53.4 in cores 17940-2 and 17964-2/3, respectively, with higher values during the last glacial than during the Holocene in both cores (Fig. 4). Species diversity expressed by the Shannon–Weaver index shows quite different patterns in both cores: it increased in core 17940-2 and decreased in core 17964-2/3 during the last glacial (Fig. 4). The changes in species diversity are negatively related to changes in the percentage of infaunal calcareous tests. Abundance fluctuations of infaunal tests are commonly related to changes in the amount of Corg reaching the seafloor and ultimately fluctuations in primary productivity (Corliss, 1985; Corliss and Chen, 1988; Rathburn and Corliss, 1994). This implies, that the species diversity decreased when primary productivity increased and a few infaunal species such as *Bulimina aculeata* and *Uvigerina peregrina* dominated (Figs. 4 and 8).

The fluctuations in the percentage of porcellaneous tests display obvious spikes in both cores

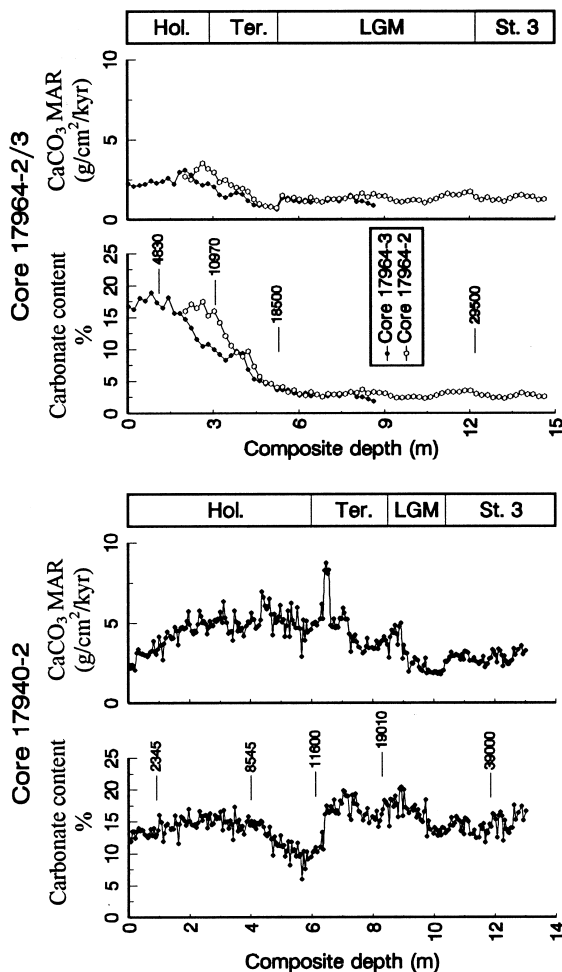


Fig. 3. Variations in carbonate content (%) and MAR ( $\text{g cm}^{-2} \text{ kyr}^{-1}$ ) in cores 17940-2 and 17964-2/3. The added lines with calendar ages are from Wang et al. (1999). Hol., Ter., LGM and St. 3 on the right side are abbreviated from Holocene, Termination I, last glacial maximum and  $\delta^{18}\text{O}$  stage 3, respectively.

during the last deglaciation, from about 18 to 10 ka B.P. (Fig. 5). However, the percentage of agglutinated tests in both cores increased during the Holocene (Fig. 5), which may be caused by taphonomic processes or enhanced carbonate dissolution. The carbonate dissolution model is supported by the increased Holocene planktonic foraminiferal fragmentation in both cores (Fig. 5), and may confirm that the SCS shares the same carbonate dissolution signals as the Pacific during the late Quaternary (Le and Shackleton, 1992).

The relative abundance data for the most common benthic foraminiferal taxa in cores 17940-2 and 17964-2/3 show major differences between glacial and Holocene periods (see Figs. 8 and 11). We used Q-mode factor analyses to better discriminate benthic foraminiferal assemblages. In core 17940-2, three varimax factors were obtained, which explain 85.0% of the total variance. Based on the down-core variations in factor loadings of each factor (Fig. 6) and the factor scores of each species or species-groups (Table 3), the *Uvigerina auberiana* assemblage representing factor 1, controls the greater part of the Holocene, except for the early Holocene. It is characterized by *U. auberiana*, *Globocassidulina subglobosa*, *Astrononion novozealandicum*, *Sphaeroidina bulloides*, and *Eggerella bradyi*. The *Chilostomella ovoidea* assemblage representing factor 2 of the last glacial stage and the deglaciation contains abundant *C. ovoidea*, *Globobulimina* spp., *Melonis barleeianum*, and *C. wuellerstorfi*, whereas the *B. aculeata* assemblage representing factor 3 of the early Holocene is characterized by *B. aculeata*, *C. pseudoungerianus* and *U. peregrina*.

In core 17964-2/3, only two varimax factors were obtained, which explain 93.6% of the total variance. Their distribution pattern clearly reflects the different paleoceanographic conditions in the last glacial stage and the Holocene (Fig. 7; Table 4). The *B. aculeata* assemblage representing factor 1 of the last glacial stage is characterized by *B. aculeata*, *U. peregrina*, *Globobulimina* spp. and *Bolivina robusta* ('high productivity' forms). The *E. bradyi*–*C. robertsonianus* assemblage representing factor 2 of the Holocene contains abundant *E. bradyi*, *C. robertsonianus*, *A. novozealandicum*, *C. wuellerstorfi*, *Cassidulina laevigata* and *Oridorsalis umbonatus* ('low productivity' forms).

## 5. Discussion

### 5.1. Control of benthic foraminiferal distribution by organic carbon flux and other factors

The comparison between benthic foraminiferal assemblages from the northern and southern slopes of the SCS allowed two groups of benthic foraminifera to be recognized, which show different behav-



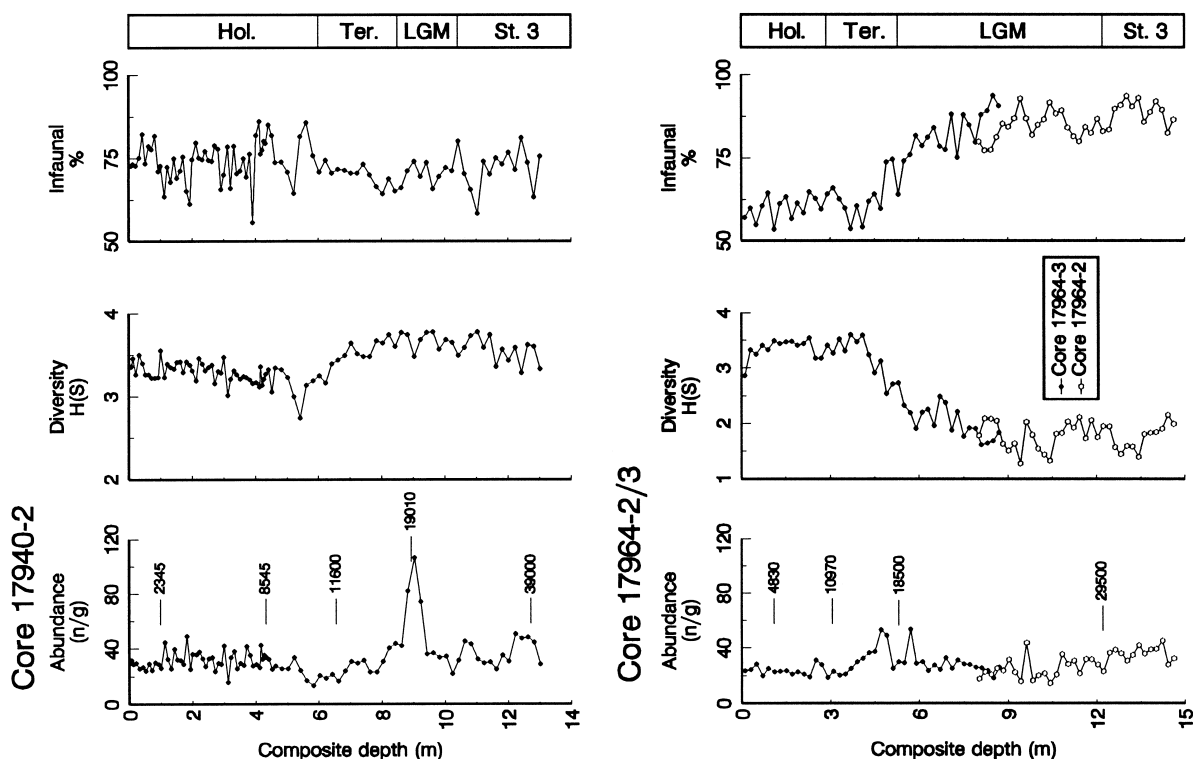


Fig. 4. Down-core variations in abundance ( $n\ g^{-1}$ ) species diversity  $H(S)$  of benthic foraminifera and relative abundance (%) of presumed infaunal taxa in cores 17940-2 and 17964-2/3. The added lines with calendar ages are from Wang et al. (1999). Hol., Ter., LGM and St. 3 on the right side are abbreviated from Holocene, Termination I, last glacial maximum and  $\delta^{18}O$  stage 3, respectively.

iors with respect to organic carbon flux. The first group exhibits fluctuations in abundance, which are clearly related to organic carbon flux. The second group also exhibits significant variations in abundance, but no correlation to carbon flux can be detected within this group.

As far as the first group is concerned, the down-core changes in the relative abundance of dominant species co-vary with independently estimated Corg flux rates (Figs. 8–10). When the Corg flux increased above  $3.5\ g\ C\ m^{-2}\ yr^{-1}$  in core 17964-2/3 during the last glacial stage before 18.5 ka B.P. and in core 17940-2 during the first part of the Holocene around 10 ka B.P., infaunal detritus feeders including *B. aculeata* and *U. peregrina* dominated. These two species reached maximum abundances of 81.5% and 48.0% in cores 17964-2/3 and 17940-2, respectively, during these periods of high organic carbon flux (Fig. 8). The accumulation rates of these two species also increased remarkably (Figs. 9 and 10).

Earlier studies often associated *Uvigerina* spp. and *B. aculeata* with low-oxygen bottom waters (Lohmann, 1978; Ingle et al., 1980; Miller and Lohmann, 1982; Sen Gupta and Machain-Castillo, 1993). However, more recent studies indicated that the abundance of these two species varies independently of the dissolved oxygen content in bottom waters (Corliss et al., 1986; Boyle, 1990; Hermelin and Shimmield, 1990; Burke et al., 1993). This was also observed in the surface sediments of the SCS (Miao et al., 1994; Rathburn and Corliss, 1994). Consequently, the glacial increase in abundances and the distributional ranges of these two species in the southeastern SCS were ascribed to an increase in sedimentary organic matter contents and surface productivity (Miao and Thunell, 1996). A similar correlation of *B. aculeata* with enhanced Corg flux was observed by Collins (1989). Our observations are in accordance with the new concept that the down-core distributions of *B. aculeata* and *U. peregrina* are controlled

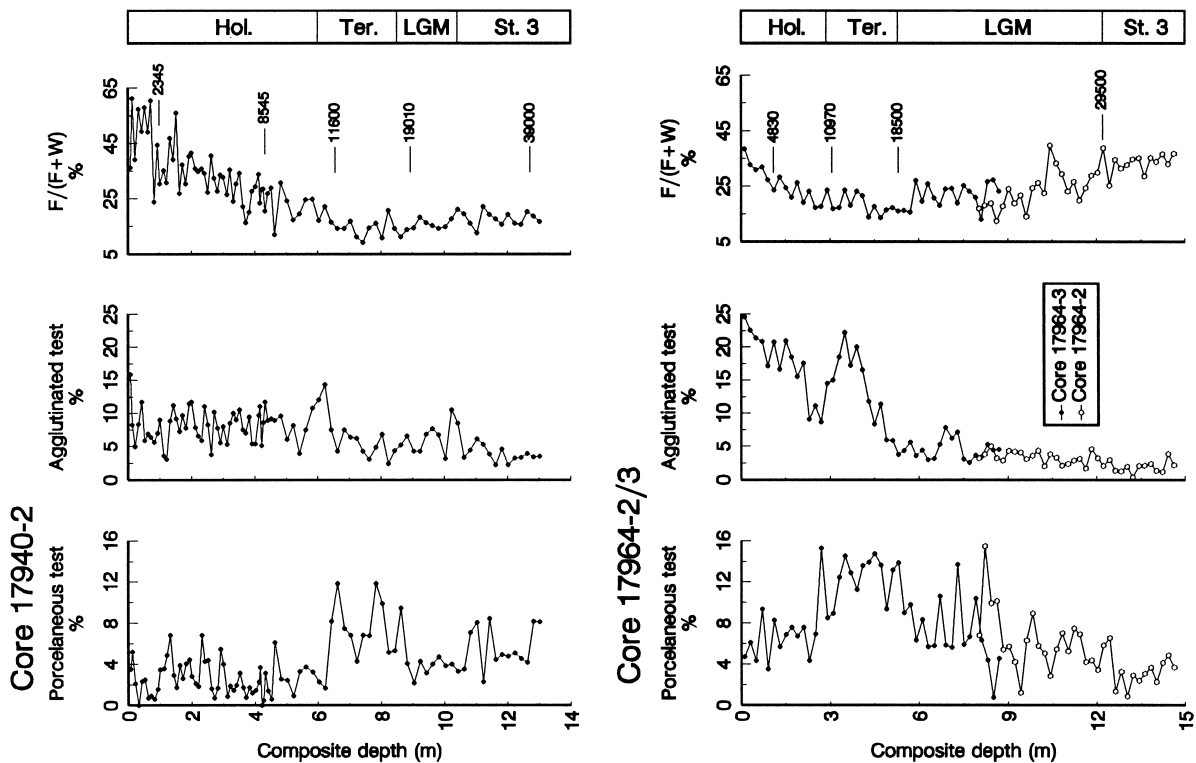


Fig. 5. Down-core variations in the ratios (%) of porcellaneous and agglutinated tests to benthic foraminiferal fauna, respectively, and planktonic foraminiferal fragmentation ( $F/(F+W)$  %) in cores 17940-2 and 17964-2/3. The added lines with calendar ages are from Wang et al. (1999). *Hol.*, *Ter.*, *LGM* and *St. 3* on the right side are abbreviated from Holocene, Termination I, last glacial maximum and  $\delta^{18}\text{O}$  stage 3, respectively.

by changing Corg flux rates towards the seafloor (Figs. 8–10; Altenbach and Sarnthein, 1989; Sarnthein and Altenbach, 1995). The increase in abundance and accumulation rate of these two species clearly indicates enhanced Corg flux and, hence increased surface export productivity during the last glacial along the southern slope and during the early Holocene along the northern slope (Figs. 8–10).

The relative abundances of suspension feeders including *C. wuellerstorfi* and a group of ‘opportunistic’ species including *O. umbonatus*, *M. barleeanum* and *C. ovoidea* (Sarnthein and Altenbach, 1995), are negatively correlated to the Corg flux in both cores (Fig. 8). Their accumulation rates, except for those of *C. wuellerstorfi* and *O. umbonatus* which are obviously controlled by other factors (see below), increased with decreased Corg flux (Fig. 9). The relative abundances and accumulation rates of these species increased during the Holocene in core

17964-2/3 and during the last glacial stage, especially during the last glacial maximum around 20–30 ka B.P. in core 17940-2 (Figs. 8 and 9). They gradually became more abundant than detritus feeders as soon as the Corg flux decreased to less than  $3.5 \text{ g C m}^{-2} \text{ yr}^{-1}$  (Fig. 8). The higher abundances of *C. wuellerstorfi* and *O. umbonatus* are widely attributed to lower Corg flux and decreased food supply associated with regions of low surface productivity (Altenbach, 1988; Burke et al., 1993; Sarnthein and Altenbach, 1995; Miao and Thunell, 1996; Kuhnt et al., 1999). *Melonis barleeanum* and *C. ovoidea* often appear to prefer higher surface productivity and high sedimentary organic contents (Lutze and Coulbourn, 1983; Ross and Kennett, 1983; Burke et al., 1993; Hermelin and Shimmield, 1995). According to our data *M. barleeanum* and *C. ovoidea* prefer lower Corg flux rates than *B. aculeata* and *U. peregrina*, i.e. less than  $3.5 \text{ g C m}^{-2} \text{ yr}^{-1}$  (Figs. 8 and 9). The

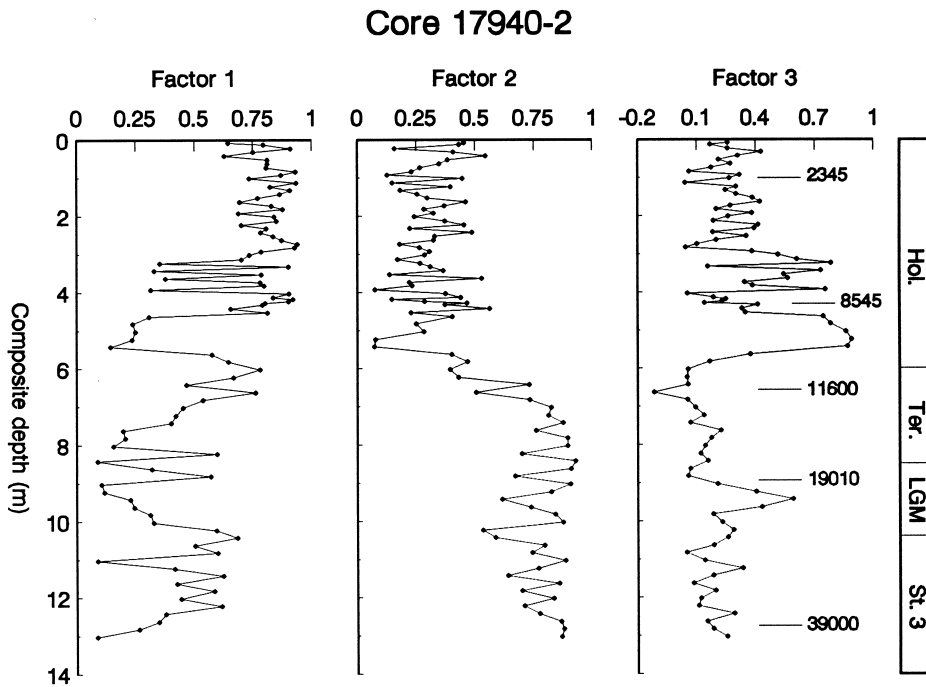


Fig. 6. Three Q-mode varimax factor loadings in core 17940-2. The added lines with calendar ages are from Wang et al. (1999). *Hol.*, *Ter.*, *LGM* and *St. 3* on the right side are abbreviated from Holocene, Termination I, last glacial maximum and  $\delta^{18}\text{O}$  stage 3, respectively.

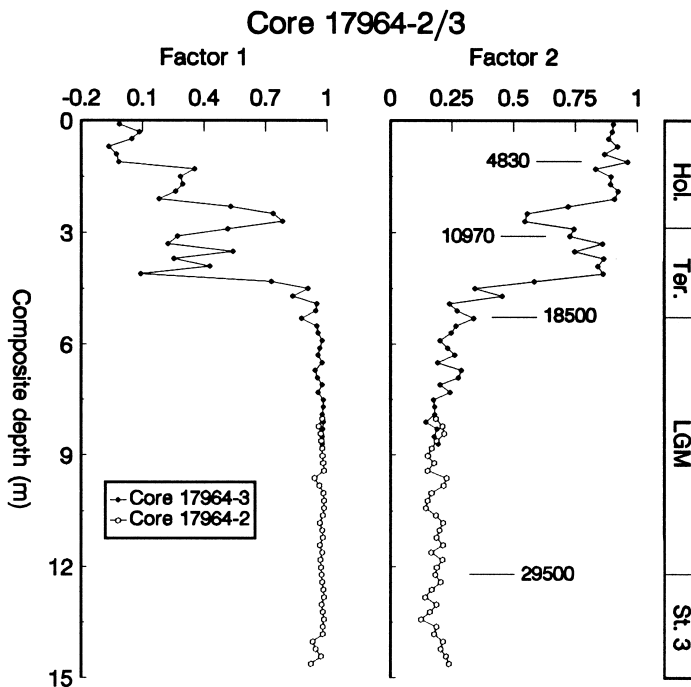


Fig. 7. Two Q-mode varimax factor loadings in core 17964-2/3. The added lines with calendar ages are from Wang et al. (1999). *Hol.*, *Ter.*, *LGM* and *St. 3* on the right side are abbreviated from Holocene, Termination I, last glacial maximum and  $\delta^{18}\text{O}$  stage 3, respectively.

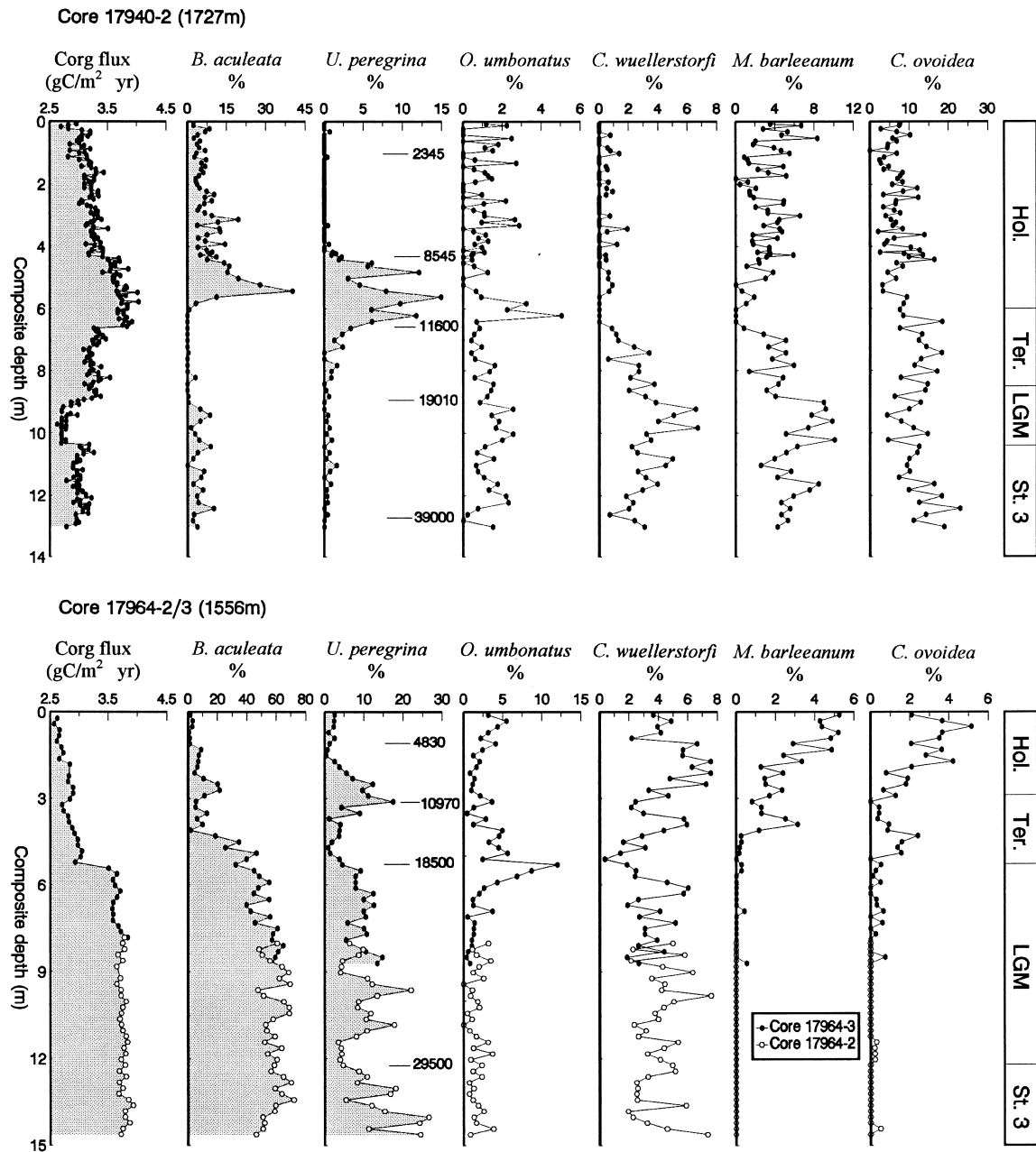


Fig. 8. Down-core variations in relative abundances of dominant benthic foraminiferal species which are clearly related to Corg flux in cores 17940-2 and 17964-2/3. The added lines with calendar ages are from Wang et al. (1999). *Hol.*, *Ter.*, *LGM* and *St. 3* on the right side are abbreviated from Holocene, Termination I, last glacial maximum and  $\delta^{18}\text{O}$  stage 3, respectively.

distribution patterns of these two major subgroups of benthic foraminifera in the SCS is obviously controlled by two different ranges of Corg flux to the seafloor ( $>3.5$  and  $2.5\text{--}3.5$   $\text{g C m}^{-2} \text{ yr}^{-1}$ ).

The abundance pattern of a second group of deep-sea benthic foraminifera in the SCS seems not to be related to Corg flux. The relative abundances of common species in this group exhibit very similar

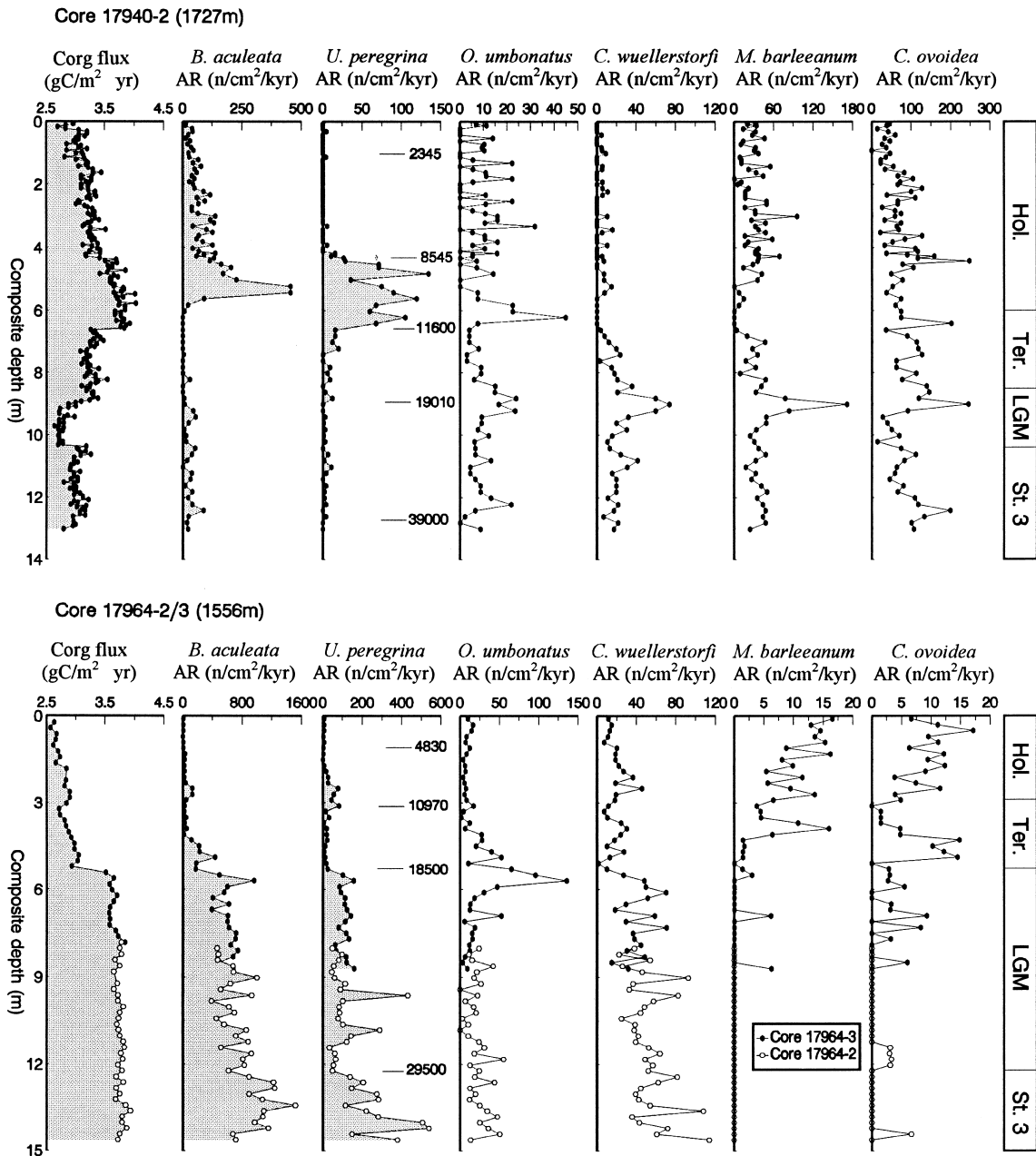


Fig. 9. Down-core variations in accumulation rates (AR) of dominant benthic foraminiferal species which are clearly related to Corg flux in cores 17940-2 and 17964-2/3. The added lines with calendar ages are from Wang et al. (1999). Hol., Ter., LGM and St. 3 on the right side are abbreviated from Holocene, Termination I, last glacial maximum and  $\delta^{18}\text{O}$  stage 3, respectively.

glacial–interglacial variation patterns in both cores 17940-2 and 17964-2/3. *E. bradyi*, *G. subglobosa*, *A. novozealandicum*, *S. bulloides*, *C. robertsonianus*, and *Cibicidoides pseudoungerianus* increased dur-

ing the Holocene and decreased during the last glacial. In contrast, *Globobulimina* spp. decreased from the last glacial to the Holocene (Fig. 11). The same productivity-independent changes in abun-

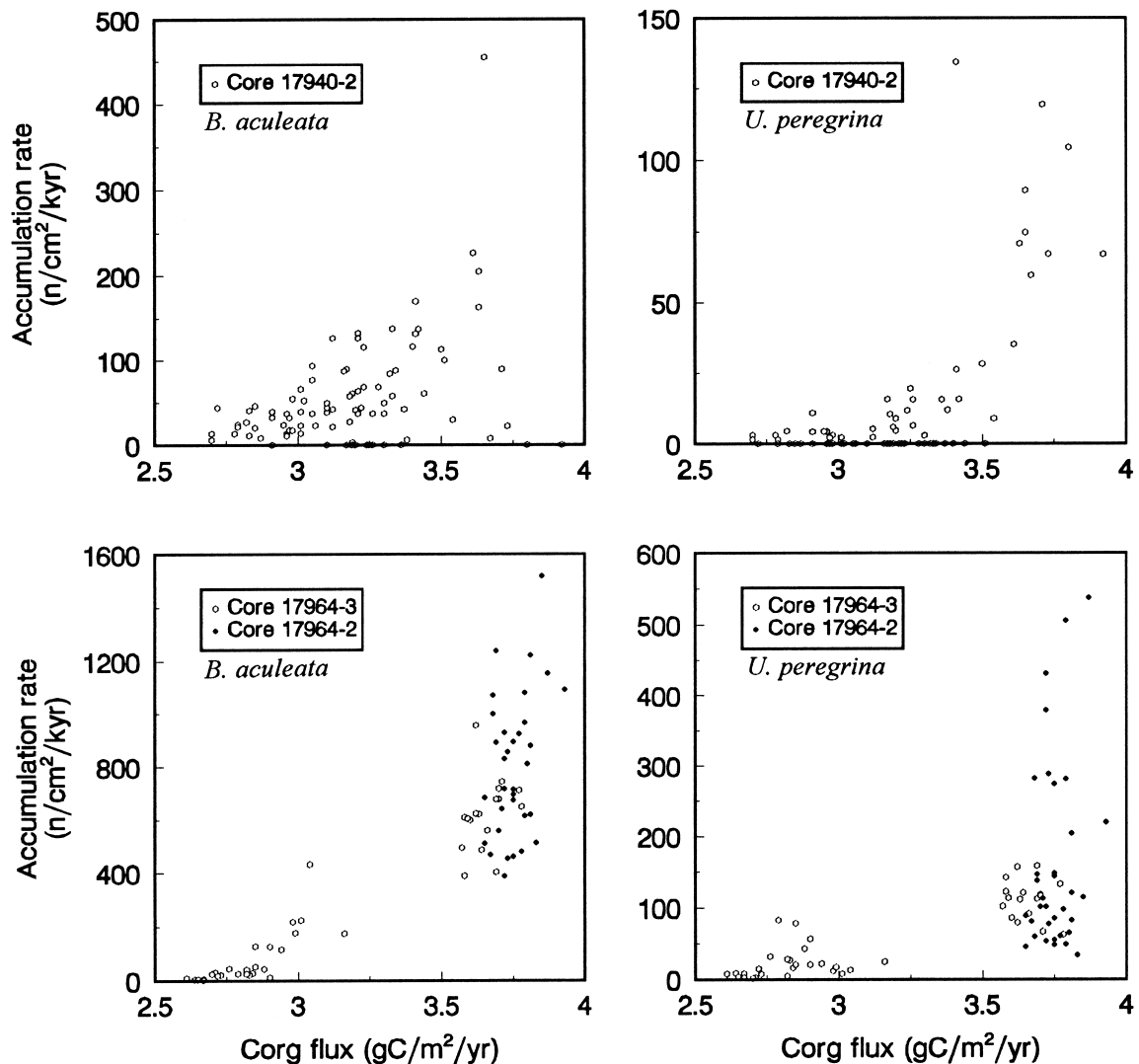


Fig. 10. Relationships of the accumulation rates of *B. aculeata* and *U. peregrina* with Corg flux in cores 17940-2 and 17964-2/3.

dances of *A. novozealandicum*, *E. bradyi*, *C. robertsonianus*, *G. subglobosa*, and *Globobulimina* spp. were reported from other areas of the SCS (Miao and Thunell, 1996; Jian and Wang, 1997), the Sulu Sea (Miao and Thunell, 1996), the western Pacific (Ujiié, 1990; Burke et al., 1993) and the Arabian Sea (Hermelin and Shimmield, 1995). With the exception of *C. pseudoungerianus*, the accumulation rates and abundances of this species group display the same glacial–interglacial variation patterns in the SCS (Fig. 12). These changes do not appear to be related to the Corg flux, since the variation patterns

of Corg fluxes are quite different in the two studied cores (Fig. 2). Other controlling factors than Corg flux, for example the properties of the ambient water masses (Hermelin and Shimmield, 1995; Miao and Thunell, 1996; Jian and Wang, 1997), may have an important influence on the distribution patterns of these species.

Various chemical and/or physical properties in intermediate- and deep-water masses are often invoked to explain changes in the species composition of deep-sea benthic foraminiferal assemblages (Streeter, 1973; Lohmann, 1978; Streeter and Shack-

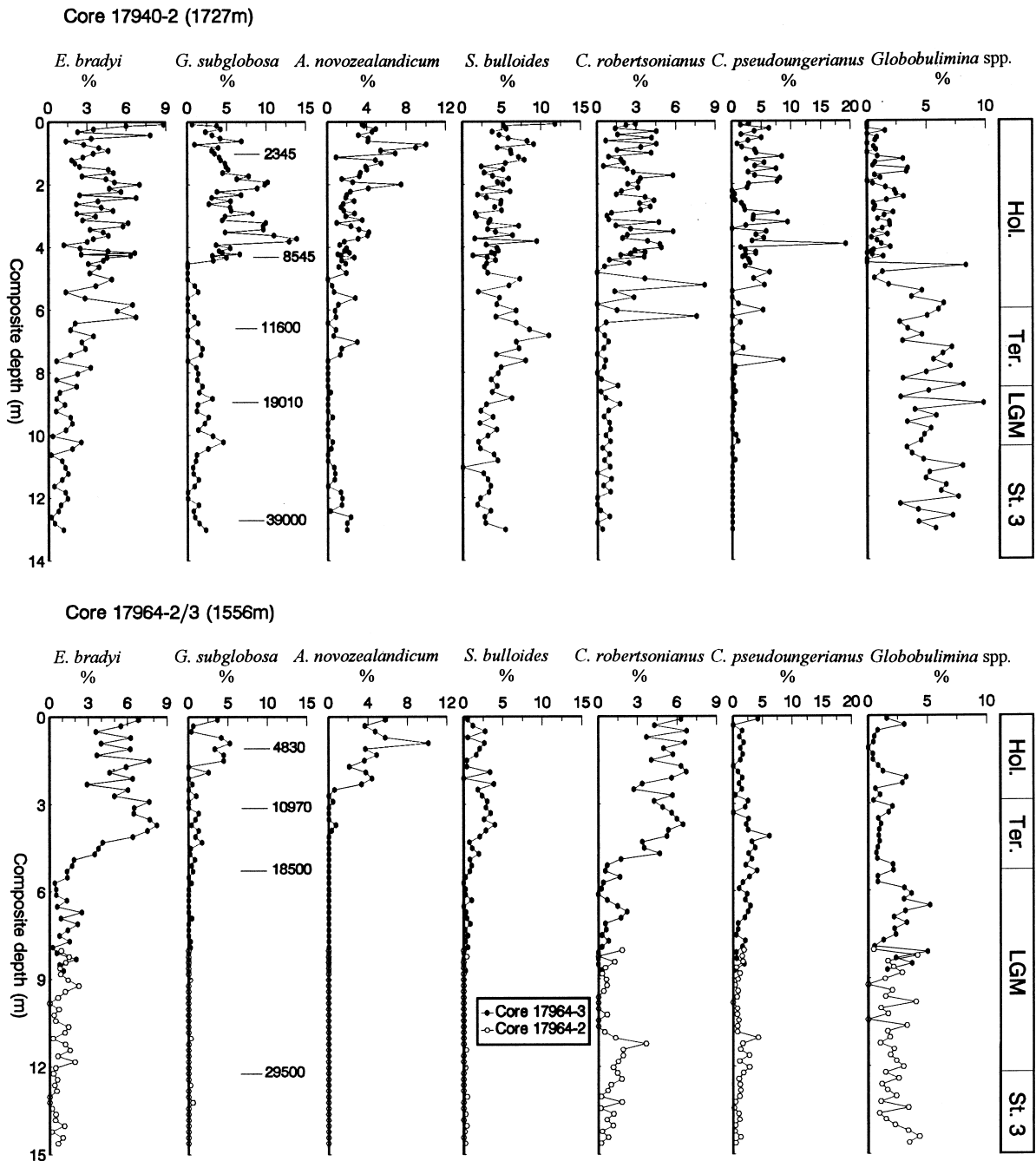


Fig. 11. Glacial–interglacial variations in relative abundances of common benthic foraminiferal species which seem not to be related to Corg flux in cores 17940-2 and 17964-2/3. The added lines with calendar ages are from Wang et al. (1999). *Hol.*, *Ter.*, *LGM* and *St. 3* on the right side are abbreviated from Holocene, Termination I, last glacial maximum and  $\delta^{18}\text{O}$  stage 3, respectively.

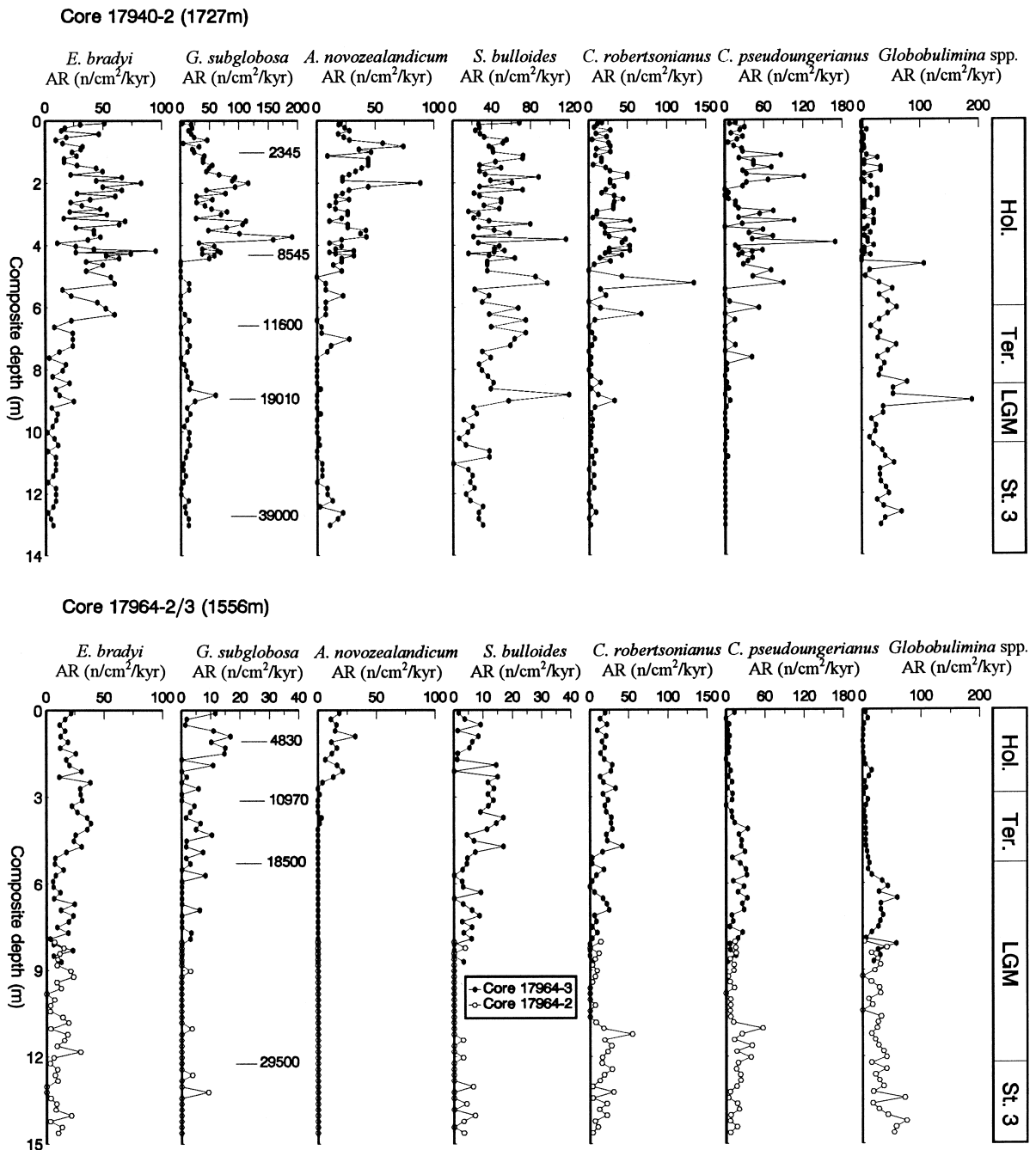


Fig. 12. Glacial–interglacial variations in accumulation rates (AR) of common benthic foraminiferal species which seem not to be related to Corg flux in cores 17940-2 and 17964-2/3. The added lines with calendar ages are from Wang et al. (1999). Hol., Ter., LGM and St. 3 on the right side are abbreviated from Holocene, Termination I, last glacial maximum and  $\delta^{18}\text{O}$  stage 3, respectively.



leton, 1979; Douglas and Woodruff, 1981; Hermelin and Shimmield, 1990; Jian and Wang, 1997). During the late Quaternary glacial cycles, the deep-water masses of the SCS were always connected to the open Pacific and experienced significant changes in chemical and physical properties (Berger, 1987; Duplessy et al., 1988; Curry et al., 1988; Le and Shackleton, 1992; Herguera, 1992; Miao and Thunell, 1996; Jian and Wang, 1997). High glacial benthic foraminiferal  $\delta^{13}\text{C}$  values during the last glacial maximum in the open Pacific at water depths between 1000 m and 2600 m suggest that nutrient-depleted deep water was produced in the North Pacific at that time (Curry et al., 1988; Duplessy et al., 1988; Shackleton et al., 1988). Based on the  $\delta^{18}\text{O}$  and  $\delta^{13}\text{C}$  differences between the LGM and Holocene in the SCS, Jian and Wang (1997) also proposed a larger contribution of cooler (about  $1^\circ\text{C}$ ) or more saline (by about 0.4‰) and better ventilated water with heavier  $\delta^{13}\text{C}$  values during the LGM than during the Holocene. This trend, however, was not confirmed by the recent high-resolution stable isotope records in cores 17940 and 17961/64 (Wang et al., 1999). In contrary, the ventilation of glacial intermediate water was much reduced at sites 17940 and 17964. The  $\text{CaCO}_3$  MAR in cores 17940-2 and 17964-2/3 displays a distinct pattern of glacial decrease and early Holocene or Termination IA/B increase, although the fluctuation patterns of carbonate contents are quite different (Fig. 3). Therefore, significant glacial–interglacial changes in the chemical and physical properties must have occurred in the ambient water mass at the locations of cores 17940-2 and 17964-2/3. These changes, probably related to the 100 kyr ice volume cycle, influenced the temperature, salinity and carbonate availability of the benthic environment and may have caused the observed fluctuations in abundances of benthic foraminiferal species.

The fluctuations in relative abundances of *C. wuellerstorfi* and *O. umbonatus* displayed opposite trends in both cores as shown by their negative correlation with the Corg flux (Fig. 8). However, the fluctuations in accumulation rates of these two species are similar in both cores, with higher values during the last glacial than during the Holocene (Fig. 9). Distinct maxima occur within Termination IA or IB. This may be explained by the observation

that the distribution of suspension feeders such as *C. wuellerstorfi* is also controlled by the intensity of bottom currents that contribute to the lateral advection of particulate nutrients (Kaminski et al., 1988; Sarnthein and Altenbach, 1995). This implies that the low accumulation rates of *C. wuellerstorfi* in the Holocene indicate weakened bottom current activity in the SCS after a short culmination in Termination IA.

A commonly underestimated difficulty in benthic foraminiferal paleoceanography is taphonomic problems (Loubere and Gray, 1990). Generally, taphonomic processes may lead to an over-estimation of infaunal species in fossil communities since tests of epifaunal species remain for a longer time within the benthic mixing zone before they can be fossilized. Infaunal species may rapidly reach the sediment below the mixing zone and get fossilized once the redox boundary moves up only a small distance (Loubere and Gray, 1990; Kuhnt et al., 1999). Additionally, many benthic foraminiferal species select their microhabitat in response to temporal and spatial variations in the Corg flux (Altenbach, 1992; Kaminski et al., 1997). The relations between changes in organic carbon flux rates, dynamic microhabitat adaptation by benthic foraminifera and taphonomy are still poorly understood, and may significantly complicate the interpretation of glacial–interglacial changes in benthic foraminiferal paleoceanography.

So far, we believe that Corg flux is the main controlling factor on the distribution of benthic foraminifera, especially in regions with important changes of surface productivity during glacial cycles, such as parts of the SCS. The intermediate- and deep-water chemical and/or physical properties may also play an important role, especially the bottom water carbonate chemistry (Hermelin and Shimmield, 1995; Miao and Thunell, 1996). However, we are still far from deciphering the influence of individual factors on the distribution of benthic foraminifera and commonly ignored factors (i.e. resource competition and predation) may even turn out to be important. Fortunately, more than 30,000 samples of 48 gravity and piston cores and 46 box cores from the slope and abyssal basin of the SCS, raised by the R/V *Sonne* in 1994 during a joint German–Chinese expedition (Sarnthein et al., 1994), provide a database to further deciphering the signal from benthic foraminifera and

to better understanding the deep-water paleoceanography of the SCS.

### 5.2. Changes in the monsoonal system over the last 40,000 years

Climate and hydrography in the SCS region are largely controlled by the monsoonal wind system which is characterized by its pronounced seasonality. Previous studies of variations in the monsoonal activity and associated upwelling concentrated on the changes in productivity recorded by planktonic and benthic foraminifera, pollen, sediment geochemistry, and isotopic composition of planktonic and benthic foraminifera in the South Asian monsoon region (Sirocko et al., 1991; Clemens et al., 1991; Hermelin and Shimmield, 1995). In the last few years, many scientists were also involved in the studies on the changes in the East Asian monsoonal system (Sarnthein et al., 1994), and some preliminary results were published elsewhere (L. Wang et al., 1995; Sun, 1995; Sarnthein et al., 1996; Wang et al., 1999).

According to the monsoonal wind system and surface circulation patterns in the SCS (P. Wang et al., 1995; Wang and Li, 1995), the main potential areas of winter monsoonal upwelling are situated at the northwestern edge of the Philippines and along the northeast–southwest running portion of the Sunda slope, whereas summer monsoonal upwelling predominates along the southeastern portion of the Vietnam margin (Sarnthein et al., 1994; Chao et al., 1996; Wiesner et al., 1996). The stable isotope curves of planktonic foraminifera (*G. ruber*), sea surface temperature records, grain size analysis of silt fraction, and pollen data in core 17940-2 show that the northeasterly winter monsoon remarkably strengthened during the last glacial before 18.0 ka B.P., while the southwesterly summer monsoon dominated during the Holocene in the SCS (Wang et al., 1999; Sun and Li, 1999). If so, can we observe significant changes in the offshore upwelling and associated productivity along the eastern margins of the SCS and do the deep-sea benthic foraminiferal fauna respond to these changes?

In core 17964-2/3 the Corg flux distinctly increased from  $<3.0$  to  $>3.5$  g C m<sup>-2</sup> yr<sup>-1</sup>, and the relative abundances and accumulation rates of *B. aculeata* and *U. peregrina* remarkably increased during

the last glacial stage just before 18.5 ka B.P. (Figs. 8 and 9). From the results of Thunell et al. (1992) and Miao and Thunell (1996), the increase in Corg flux and relative abundances of *B. aculeata* and *U. peregrina* during the last glacial should be a common phenomenon in the southern and southeastern SCS, indicating extremely high glacial fertility and surface productivity (Fig. 8). These changes would result in an increased CO<sub>2</sub>-content of the bottom waters and a depleted benthic foraminiferal  $\delta^{13}\text{C}$  caused by the oxidation of organic matter.

The negative  $\delta^{13}\text{C}$  excursions (up to  $-1.6\text{‰}$ ) of the benthic foraminifera *C. wuellerstorfi* in core 17964-2/3 within the last glacial (Fig. 13) were much greater than the excursions recorded in the open Pacific and other areas in the SCS. According to Duplessy et al. (1988), Curry et al. (1988) and Jian and Wang (1997), high glacial benthic foraminiferal  $\delta^{13}\text{C}$  values in the open Pacific and the SCS at water depths of 1000 m to 2500 m suggest that nutrient-depleted, less corrosive deep water was being produced in the North Pacific at that time. Herguera et al. (1992) also proposed that Pacific waters above 2000 m were better ventilated during the last glacial than at present. As core 17964-2/3 is located at the present water depth of 1556 m, the lowered sea level during the last glacial would not have had a significant impact on the exchange of deep water between the SCS and Pacific. Therefore, the glacial  $\delta^{13}\text{C}$  depletion at site 17964 was probably not a result of restricted deep-water circulation.

A local scenario, involving seasonal enhanced offshore upwelling driven by intensified winter monsoonal activity and a resulting rapid flux of Corg flux to the seafloor, leading to seasonal oxygen-deficient bottom conditions, can be used to explain the mid-depth deposition of organic-rich sediments and benthic  $\delta^{13}\text{C}$  depletion during the last glacial in the southern SCS. Moreover, the lowered glacial sea level may have increased terrigenous nutrient-flux to the southern slope (Broecker et al., 1988; Schönfeld and Kudrass, 1993; P. Wang et al., 1995), may have further enhanced surface productivity, and induced poor ventilation as a result of a more vigorous estuarine system. The glacial  $\delta^{13}\text{C}$  of Corg were lighter than the Holocene values (M. Sarnthein and M. Kienast, unpubl. data), suggesting that the increased terrigenous carbon deposition was at least partly re-

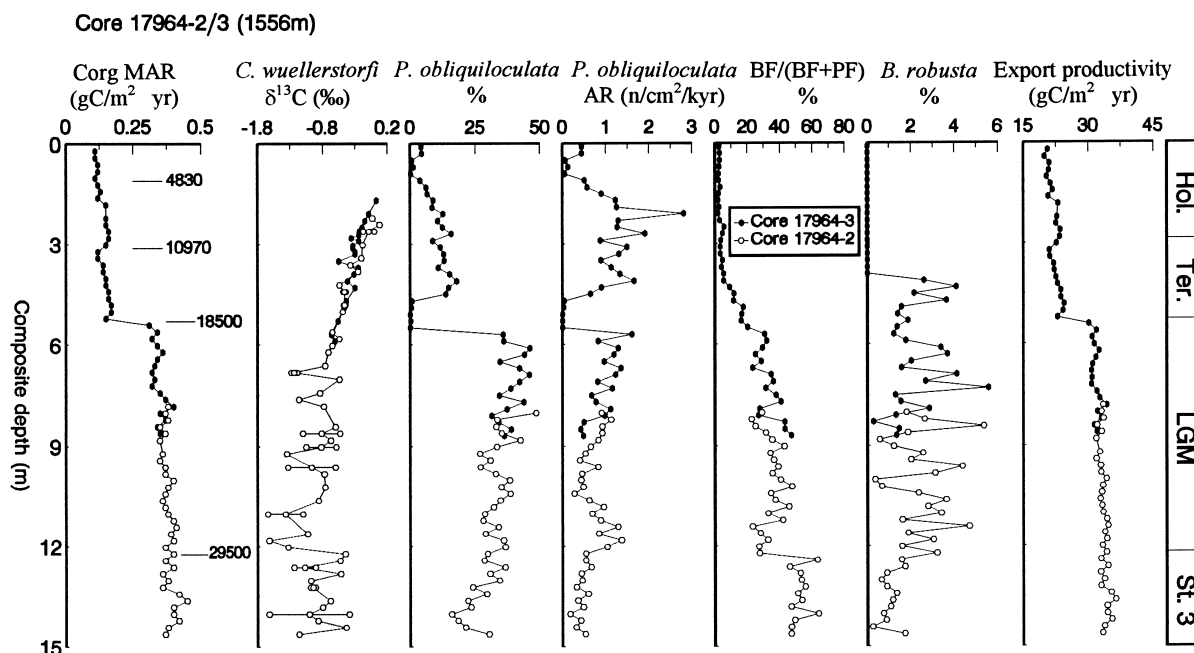


Fig. 13. Curves of Corg MAR,  $\delta^{13}\text{C}\%$  of *C. wuellerstorfi*, relative abundances of *P. obliquiloculata* and *B. robusta*, accumulation rates (AR) of *P. obliquiloculata*, BF/(BF + PF) % and export productivity in core 17964-2/3. The added lines with calendar ages are from Wang et al. (1999). Hol., Ter., LGM and St. 3 on the right side are abbreviated from Holocene, Termination I, last glacial maximum and  $\delta^{18}\text{O}$  stage 3, respectively.

responsible for the high glacial Corg flux (Thunell et al., 1992; Winn et al., 1992).

Seasonally oxygen-deficient bottom conditions in the glacial southern SCS resulted in the high relative abundance of *Bolivina robusta* which is tolerant to low-oxygen conditions (Linsley et al., 1985; Miao and Thunell, 1996) (Fig. 13). The seasonal oxygen minimum also enhanced carbonate dissolution which was reflected in (1) the remarkable increase in the benthic/planktonic foraminiferal ratio (BF/(BF + PF) %) as high as 60% (Fig. 13), (2) the abnormally high relative abundance of dissolution-resistant planktonic species *Pulleniatina obliquiloculata*, in comparison to its medium high accumulation rates (Fig. 13), and (3) the higher planktonic foraminiferal fragmentation (F/(F + W) %) (Fig. 5). In addition to the high glacial Corg flux, other factors may have played a role in the changes of dissolved oxygen content of bottom water and relative abundances of *P. obliquiloculata*. During glacial times the Sunda shelf was exposed as a result of the lowered sea level, and rivers crossed the entire shelf and entered

the southern slope of the SCS much closer to the present position of core 17964-2/3 (Fig. 1). Thus, a low-salinity surface layer in the southern SCS during the last glacial may have caused further stratification of an already seasonally oxygen-deficient water column. Additionally, the dominance of the deep-dwelling planktonic species *P. obliquiloculata* at the cost of stenohaline planktonic foraminifera in near-surface habitats (for example, *G. ruber* and *G. sacculifer*) may be explained by a low-salinity surface layer. Linsley et al. (1985) concluded that an expansion or intensification of the mid-water oxygen minimum occurred between approximately 1600 and 2050 m in the Sulu Sea during the last glacial sea-level low stand, based on the benthic  $\delta^{13}\text{C}$  depletion ( $-1.8\%$ ) and increased relative abundance of *B. robusta*. It seems that the southern SCS and Sulu Sea have experienced similar climatic and geographic changes (Linsley et al., 1985; Miao and Thunell, 1996).

The Corg flux in core 17940-2 increased after the last glacial maximum and reached its highest values

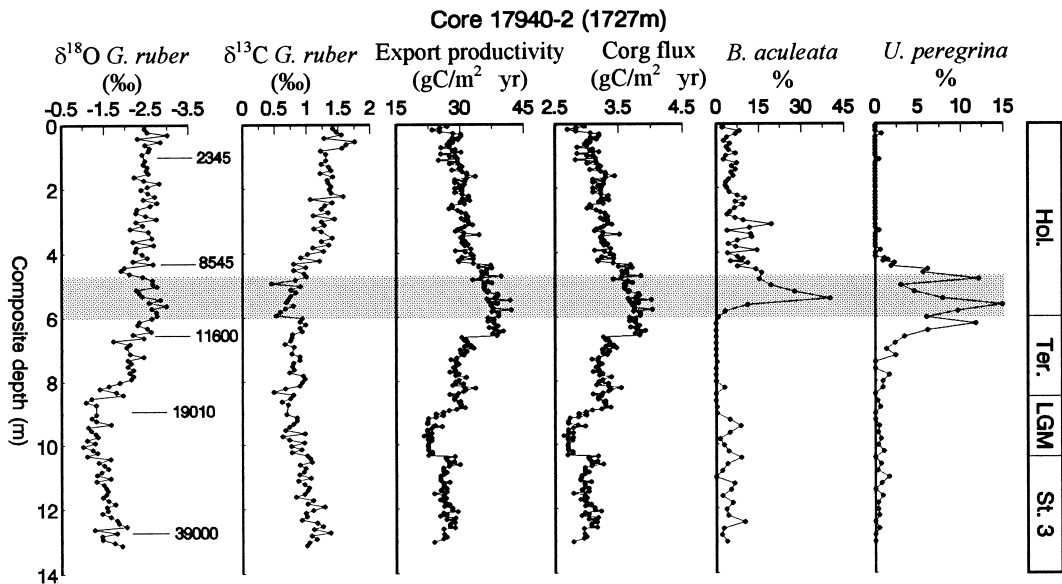


Fig. 14. Curves of  $\delta^{18}\text{O}$  and  $\delta^{13}\text{C}$  of *G. ruber* (Wang et al., 1999), Corg flux, export productivity and relative abundances of *B. aculeata* and *U. peregrina* in core 17940-2. The early Holocene maximum in summer monsoonal intensity is shaded. The added lines with calendar ages are from Wang et al. (1999). *Hol.*, *Ter.*, *LGM* and *St. 3* on the right side are abbreviated from Holocene, Termination I, last glacial maximum and  $\delta^{18}\text{O}$  stage 3, respectively.

(>3.5  $\text{g C m}^{-2} \text{ yr}^{-1}$ ) in the first part of the Holocene around 10 ka B.P. By contrast, in core 17964-2/3 the Corg flux rapidly decreased to less than 3.0  $\text{g C m}^{-2} \text{ yr}^{-1}$  right at the end of the last glacial maximum (Fig. 2). Simultaneously, the relative abundances and accumulation rates of *B. aculeata* and *U. peregrina* increased remarkably in core 17940-2 during the early Holocene (Figs. 8 and 14).

There are minima in both the  $\delta^{18}\text{O}$  and  $\delta^{13}\text{C}$  of the planktonic foraminifera *G. ruber* in core 17940-2 during the early Holocene, pointing to relatively low surface salinity as well as increased fertility (Fig. 14). These features led L. Wang et al. (1995) and Sarnthein et al. (1996) to infer a phase of increased monsoonal precipitation and fluvial runoff in the northern SCS. In the northern Indian Ocean, Kutzbach (1981), Sirocko et al. (1991) and Clemens et al. (1991) indicated an enhanced SW summer monsoon during the last deglaciation, with a maximum of offshore upwelling and minimum of surface salinity around 11,000 years ago. This enhanced SW summer monsoon is associated with the early Holocene maximum in solar insolation linked to orbital forcing. Since the Asian monsoon system

controls the climate of both East Asia and the northern Indian Ocean, similar fluctuations in monsoonal activity might be expected (Duplessy, 1982; Linsley et al., 1985; Sarnthein et al., 1996). Certainly, the increased freshwater discharge from South China due to the enhanced summer monsoon precipitation, which was concurrent with maximum freshwater input from the Indus river (Sirocko et al., 1993), could supply more terrigenous nutrients to the northern SCS and helped to increase surface productivity. This mechanism may also have functioned on the southern slope, as recorded by the minor increase in Corg flux and relative abundances of *B. aculeata* and *U. peregrina* in core 17964-2/3 during the Younger Dryas and earliest Holocene (Fig. 8), although the amplitudes of their variations are much more outstanding along the northern slope.

## 6. Conclusions

(1) The distribution patterns and accumulation rates of some deep-sea benthic foraminiferal species are primarily controlled by Corg flux to the seafloor

in the SCS. Two major subgroups of these species serve as proxy to distinguish two different ranges of Corg flux ( $>2.5$  and  $>3.5$  g C m<sup>-2</sup> yr<sup>-1</sup>). When Corg flux increases above 3.5 g C m<sup>-2</sup> yr<sup>-1</sup> in the southern SCS during the LGM and in the northern SCS during the early Holocene, a group of detritus feeders such as *B. aculeata* and *U. peregrina* dominates. Furthermore, the suspension feeders such as *C. wuellerstorfi* and ‘opportunistic’ species such as *O. umbonatus*, *M. barleeanum* and *C. ovoidea* gradually become more important than detritus feeders as soon as the Corg flux decreases to 2.5–3.5 g C m<sup>-2</sup> yr<sup>-1</sup>.

(2) A number of benthic foraminiferal species including *E. bradyi*, *G. subglobosa*, *A. novozealandicum*, *S. bulloides* and *C. robertsonianus* display very similar glacial–interglacial changes in relative abundance and accumulation rate, despite the relatively different variation patterns in Corg flux in the southern and northern SCS, perhaps responding to changes in chemical and/or physical properties of the ambient water mass.

(3) The high Corg flux and increased abundances and accumulation rates of *B. aculeata* and *U. peregrina* during the LGM in the southern SCS may be partly caused by the enhanced NE winter monsoon-driven upwelling and associated productivity, and partly by the increased input of terrigenous nutrients as a result of the lowered sea level and enhanced riverine runoff. This seasonal increase in Corg flux would have inevitably led to decreased oxygen content in bottom water and hence enhanced carbonate

dissolution, as indicated by the very low benthic  $\delta^{13}\text{C}$ , the high BF/(BF + PF) %, and the relatively high abundance of *B. robusta* in oxygen-poor habitats and dissolution-resistant *P. obliquiloculata*.

(4) During the first part of the Holocene, around 10 ka B.P., the remarkably increased abundances and accumulation rates of *B. aculeata* and *U. peregrina* especially in the northern part of the SCS, together with the high Corg flux and the minima in both the  $\delta^{18}\text{O}$  and  $\delta^{13}\text{C}$  of the planktonic foraminifera *G. ruber*, point to lower salinity as well as increased productivity, probably driven by riverine runoff as a result of a maximum intensity in the SW summer monsoon (Wang et al., 1999).

### Acknowledgements

We would like to thank the crew and scientists aboard the R/V *Sonne* for assistance during cruise 95; E. Erlenkeuser provided the stable isotope data (Wang et al., 1999); A.V. Altenbach and S. Hess are thanked for helpful discussion. A. Holbourn improved the English and helped to clarify our thoughts. A.V. Altenbach, and an anonymous reviewer reviewed the manuscript and their comments, suggestions, and constructive criticisms greatly improved the manuscript. Our research was supported by the BMBF of Germany and the National Natural Science Foundation of China (grants 49776290 and 49732060).











## References

- Altenbach, A.V., 1988. Deep-sea benthic foraminifera and flux rate of organic carbon. *Rev. Paleobiol.* 2, 719–720.
- Altenbach, A.V., 1992. Short term processes and patterns in the foraminiferal response to organic flux rates. *Mar. Micropaleontol.* 19, 119–129.
- Altenbach, A.V., Sarnthein, M., 1989. Productivity record in benthic foraminifera. In: Berger, W.H., Smetacek, V.S., Wefer, G. (Eds.), *Productivity of the Ocean: Present and Past*. Wiley, New York, Dahlem-Konferenzen, pp. 255–269.
- Bard, E., Hamelin, B., Fairbanks, R.G., Zindler, A., 1990. Calibration of the  $^{14}\text{C}$  timescale over the past 30,000 years using mass spectrometric U–Th ages from Barbados corals. *Nature* 345, 405–410.
- Barker, R.W., 1960. Taxonomic notes on the species figured by H.B. Brady in his report on the foraminifera dredged by H.M.S. 'Challenger' during the years 1873–1876. *Soc. Econ. Paleontol. Mineral. Spec. Publ.* 9, 238 pp.
- Berger, W.H., 1987. Ocean ventilation during the last 12,000 years: hypothesis of counterpoint deep water production. *Mar. Geol.* 78, 1–10.
- Boyle, E.A., 1990. Quaternary deepwater paleoceanography. *Science* 247, 863–869.
- Broecker, W.S., Andree, M., Klas, M., Bonani, G., Wolff, W., Oeschger, H., 1988. New evidence from the South China Sea for an abrupt termination of the last glacial period. *Nature* 333, 156–158.
- Burke, S.K., Berger, W.H., Coulbourn, W.T., Vincent, E., 1993. Benthic foraminifera in box core ERDC 112, Ontong Java Plateau. *J. Foraminiferal Res.* 23 (1), 19–39.
- Chao, S.-Y., Shaw, P.-T., Wu, S.Y., 1996. Deep water ventilation in the South China Sea. *Deep-Sea Res. (Part A)* 43 (4), 445–466.
- Clemens, S., Prell, W., Murray, D., Shimmield, G., Weedon, G., 1991. Forcing mechanisms of the Indian Ocean monsoon. *Nature* 353, 720–725.
- Collins, L.S., 1989. Relationship of environmental gradients to morphologic variation within *Bulimina aculeata* and *Bulimina marginata*, Gulf of Maine Area. *J. Foraminiferal Res.* 19 (3), 222–234.
- Corliss, B.H., 1985. Microhabitats of benthic foraminifera within deep-sea sediments. *Nature* 314, 435–438.
- Corliss, B.H., 1994. The ecology of deep-sea benthic foraminifera. *Peleobios* 16 (2) Supplements, 28.
- Corliss, B.H., Chen, C., 1988. Morphotype patterns of Norwegian Sea deep-sea benthic foraminifera and ecological implications. *Geology* 16, 716–719.
- Corliss, B.H., Martison, D.G., Keffer, T., 1986. Late Quaternary deep-ocean circulation. *Geol. Soc. Am. Bull.* 97, 1106–1121.
- Curry, W.B., Duplessy, J.C., Labeyrie, L.D., Shackleton, N.J., 1988. Quaternary deep-water circulation changes in the distribution of  $\delta^{13}\text{C}$  of deep water  $\Sigma\text{CO}_2$  between the last glaciation and the Holocene. *Paleoceanography* 3 (3), 317–342.
- Douglas, R., Woodruff, F., 1981. Deep-sea benthic foraminifera. In: Emiliani, C. (Ed.), *The Sea, The Oceanic Lithosphere*, 1. Wiley, New York, pp. 1233–1328.
- Duplessy, J.C., 1982. Glacial to interglacial contrasts in the northern Indian Ocean. *Nature* 295, 496–498.
- Duplessy, J.C., Shackleton, N.J., Fairbanks, R.G., Labeyrie, L., Oppo, D., Kallel, N., 1988. Deepwater source variations during the last climatic cycles and their impact on the global deepwater circulation. *Paleoceanography* 3 (3), 343–360.
- Herguera, J.C., 1992. Deep-sea benthic foraminifera and biogenic opal: glacial to post-glacial productivity changes in the western equatorial Pacific. *Mar. Micropaleontol.* 19, 79–98.
- Herguera, J.C., Jansen, E., Berger, W., 1992. Evidence for a bathyal front at 200 m depth in the glacial Pacific, based on a depth transect on the Ontong Java Plateau. *Paleoceanography* 7, 273–288.
- Hermelin, J.O.R., Shimmield, G.B., 1990. The importance of the oxygen minimum zones and sediment geochemistry in the distribution of Recent benthic foraminifera in the Northwest Indian Ocean. *Mar. Geol.* 91, 1–29.
- Hermelin, J.O.R., Shimmield, G.B., 1995. Impact of productivity events on the benthic foraminiferal fauna in the Arabian Sea over the last 150,000 years. *Paleoceanography* 10 (1), 85–116.
- Ingle, J.C., Keller, G., Kolpach, R.L., 1980. Benthic foraminiferal biofacies, sediments and water masses of the southern Peru–Chili Trench area, Southern Pacific Ocean. *Micropaleontology* 26 (2), 113–150.
- Jian, Z., Wang, L., 1997. Late Quaternary benthic foraminifera and deep-water paleoceanography in the South China Sea. *Mar. Micropaleontol.* 32, 127–154.
- Jian, Z., Zheng, L., 1992. Benthic foraminifera in surface sediments and the deeper water masses of the central South China Sea (in Chinese, with English abstr.). In: Ye, Z., Wang, P. (Eds.), *Contributions to Late Quaternary Paleoceanography of the South China Sea*. Qingdao Ocean University Press, Qingdao, pp. 140–155.
- Kaminski, M.A., Grassle, J.F., Whitlatch, R.B., 1988. Life history and recolonisation among agglutinated foraminifera in the Panama basin. In: Grastein, N.F., Rögel, F. (Eds.), *Second Workshop on Agglutinated Foraminifera*. Abh. Geol. Bundesanst. (Wien) 41, 229–243.
- Kaminski, M.A., Al Hassawi, A.M., Kuhnt, W., 1997. Seasonality in microhabitats of Rose Bengal stained deep-sea benthic foraminifera from the New Jersey continental margin. In: Gryzbowski Foundation Spec. Publ. 5, in press.
- Klovan, J.E., Imbrie, J., 1971. An algorithm and FORTRAN IV program for large scale Q-mode factor analysis. *Int. Assoc. Math. Geol. J.* 3, 61–78.
- Kuhnt, W., Hess, S., Jian, Z., 1999. Quantitative composition of benthic foraminiferal assemblages as a proxy indicator for organic carbon flux rates in the South China Sea. *Mar. Geol.* 156, 123–158.
- Kutzbach, J.E., 1981. Monsoon climate of the early Holocene: climate experiment with the earth's orbital parameters for 9000 years ago. *Science* 214, 59–61.
- Le, J., Shackleton, N.J., 1992. Carbonate dissolution fluctuations in the western equatorial Pacific during the late Quaternary. *Paleoceanography* 7 (1), 21–42.

- Linsley, B.K., Thunell, R.C., Morgan, C., Williams, D.F., 1985. Oxygen minimum expansion in the Sulu Sea, Western Equatorial Pacific, during the Last Glacial low stand of sea level. *Mar. Micropaleontol.* 9, 395–418.
- Lohmann, G.P., 1978. Abyssal benthic foraminifera as hydrographic indicators in the western South Atlantic Ocean. *J. Foraminiferal Res.* 8 (1), 6–34.
- Loubere, P., Gray, A., 1990. Taphonomic process and species microhabitats in the living to fossil assemblage transition of deeper water benthic foraminifera. *Palaios* 5, 375–381.
- Lutze, G.F., 1980. Depth distribution of benthic foraminifera on the continental margin off northwest Africa. *'Meteor' Forschungsergeb. Reihe C* 32, 31–80.
- Lutze, G.F., Coulbourn, W.T., 1983. Recent benthic foraminifera from the continental margin of northwest Africa: community structures and distribution. *Mar. Micropaleontol.* 8, 361–401.
- Miao, Q., Thunell, R.C., 1993. Recent deep-sea benthic foraminiferal distribution in the South China Sea. *Mar. Micropaleontol.* 22, 1–32.
- Miao, Q., Thunell, R.C., 1996. Late Pleistocene–Holocene distribution of deep-sea benthic foraminifera in the South China Sea and Sulu Sea: paleoceanographic implications. *J. Foraminiferal Res.* 26 (1), 9–23.
- Miao, Q., Thunell, R.C., Anderson, D.M., 1994. Glacial–Holocene paleoceanography of the western equatorial Pacific Ocean: carbonate dissolution and sea surface temperature in the South China and Sulu Seas. *Paleoceanography* 9, 69–90.
- Miller, H.G., Lohmann, G.P., 1982. Environmental distribution of Recent benthic foraminifera on the northeast United States continental slope. *Geol. Soc. Am. Bull.* 93, 200–206.
- Pearson, G.W., Becker, B., Qua, F., 1993. High-precision  $^{14}\text{C}$  measurement of German and Irish oaks to show the natural  $^{14}\text{C}$  variations from 7890 to 5000 BC. *Radiocarbon* 35 (1), 93–104.
- Rathburn, A.E., Corliss, B.H., 1994. The ecology of living (stained) deep-sea benthic foraminifera from the Sulu Sea. *Paleoceanography* 9, 87–150.
- Ross, C.R., Kennett, J.P., 1983. Late Quaternary paleoceanography as recorded by benthic foraminifera in Strait of Sicily sediment sequences. *Mar. Micropaleontol.* 8, 315–326.
- Saidova, Kh.M., 1975. Benthic Foraminifera of the Pacific Ocean. *Acad. Sci. USSR, P.P. Shirshor Inst. Oceanogr., Moscow*, 631 pp.
- Sarnthein, M., Altenbach, A.V., 1995. Late Quaternary changes in surface water and deep water masses of the Nordic Seas and north-eastern North Atlantic: a review. *Geol. Rundsch.* 84, 89–107.
- Sarnthein, M., Pflaumann, U., Ross, R., Tiedemann, R., Winn, K., 1992. Transfer functions to reconstruct ocean paleoproductivity: a comparison. In: Summerhayes, C.P., Prell, W.L., Emeis, K.C. (Eds.), *Upwelling Systems: Evolution since the Early Miocene*. *Geol. Soc. London, Spec. Publ.* 64, 411–427.
- Sarnthein, M., Pflaumann, U., Wang, P., Wong, H.K. (Eds.), 1994. Preliminary Report on SONNE-95 Cruise 'Monitor Monsoon' to the South China Sea. *Berichte-Reports, Geol. Paleontol. Inst. Univ. Kiel* 68, 225 pp.
- Sarnthein, M., Wang, L., Heilig, S., Lin, H.L., Ivanova, E., Jian, Z., Kienast, M., Pelejero, C., Pflaumann, U., 1996. Response of East Asian monsoonal climate to orbital forcing and fluctuations of the ocean salinity conveyor belt: high-resolution records from the South China Sea. In: *Abstracts of 30th International Geological Congress, Beijing*, 2, p. 251.
- Schönfeld, J., Kudrass, H.R., 1993. Hemipelagic sediment accumulation rates in the South China Sea related to late Quaternary sea-level changes. *Quat. Res.* 40, 368–379.
- Sen Gupta, B.K., Machain-Castillo, M., 1993. Benthic foraminifera in oxygen-poor habitats. *Mar. Micropaleontol.* 20, 183–201.
- Shackleton, N.J., Duplessy, J.C., Arnold, M., Maurice, P., Hall, M.A., Cartlidge, J., 1988. Radiocarbon age of last glacial Pacific deep water. *Nature* 335, 708–711.
- Sirocko, F., Sarnthein, M., Lange, H., Erlenkeuser, H., 1991. Atmospheric summer circulation and coastal upwelling in the Arabian Sea during the Holocene and the last glaciation. *Quat. Res.* 36, 72–93.
- Sirocko, F., Sarnthein, M., Erlenkeuser, H., Lange, H., Arnold, M., Duplessy, J.C., 1993. Century-scale events in monsoonal climate over the past 24,000 years. *Nature* 364, 322–324.
- Streeter, S.S., 1973. Bottom water and benthic foraminifera in the North Atlantic glacial–interglacial contrasts. *Quat. Res.* 3, 131–141.
- Streeter, S.S., Shackleton, N.J., 1979. Paleocirculation of the deep North Atlantic: 150,000 year record of benthic foraminifera and oxygen-18. *Science* 203, 168–170.
- Stuiver, M., Becker, B., 1993. High-precision decadal calibration of the radiocarbon time scale, AD 1950–6000 BC. *Radiocarbon* 35 (1), 35–65.
- Stuiver, M., Braziunas, T.F., 1993. Modeling atmospheric  $^{14}\text{C}$  influences and  $^{14}\text{C}$  ages of marine samples to 10,000 BC. *Radiocarbon* 35 (1), 137–189.
- Sun, X., 1995. Paleoenvironmental evolution recorded by deep-sea pollen in the South China Sea (in Chinese). In: Wang, P. (Ed.), *The South China Sea during the last 150,000 Years*. *Tongji University Press, Shanghai*, pp. 65–74.
- Sun, X., Li, X., 1999. Pollen records of the last 37 ka in deep-sea core 17940 from the northern slope of the South China Sea. *Mar. Geol.* 156, 227–244.
- Thomas, E., Booth, L., Maslin, M., Shackleton, N.J., 1995. Northeastern Atlantic benthic foraminifera during the last 45,000 years: changes in productivity seen from the bottom up. *Paleoceanography* 10 (3), 545–562.
- Thunell, R.C., 1976. Optimum indices of calcium carbonate dissolution in deep-sea sediments. *Geology* 4, 525–527.
- Thunell, R.C., Miao, Q., Calvert, S.E., Pedersen, T.F., 1992. Glacial–Holocene biogenic sedimentation patterns in the South China Sea: productivity variations and surface water  $p\text{CO}_2$ . *Paleoceanography* 7, 143–162.
- Tu, X., 1983. Distribution and habitats of foraminifera in surface sediments of the northern South China Sea (in Chinese, with English abstr.) *Tropical Oceanol.* 2 (1), 11–19.
- Ujjié, H., 1990. Bathyal benthic foraminifera in a piston core east off the Miyako Islands, Ryukyu Island Arc. *Bull. Coll. Sci. Univ. Ryukyus* 49, 60 pp.
- Wang, L., Wang, P., 1990. Late Quaternary paleoceanography of

- the South China Sea: glacial–interglacial contrasts in enclosed basin. *Paleoceanography* 5, 77–90.
- Wang, L., Pflaumann, U., Sarnthein, M., 1995. High-resolution sediment records of climatic change in the South China Sea during the last 30,000 years. In: Program and Abstracts of 5th International Conference on Paleocyanography. Halifax, pp. 175–176.
- Wang, L., Sarnthein, M., Erlenkeuser, H., Grimalt, J., Grootes, P., Heilig, S., Ivanova, E., Pelejero, C., Pflaumann, U., 1999. East Asian monsoon climate during the Late Pleistocene: high-resolution sediment records from the South China Sea. *Mar. Geol.* 156, 245–284.
- Wang, P., 1990. The Ice-Age China Sea — research results and problems. In: Wang, P., Lao, Q., He, Q. (Eds.), *Proc. 1st Int. Conf. Asian Marine Geology*. China Ocean Press, Beijing, pp. 181–197.
- Wang, P., Li, R., 1995. Numerical simulation of surface circulation of South China Sea during the last glaciation and its verification. *Chin. Sci. Bull.* 40 (21), 1813–1817.
- Wang, P., Wang, L., Bian, Y., Jian, Z., 1995. Late Quaternary paleoceanography of the South China Sea: surface circulation and carbonate cycles. *Mar. Geol.* 127, 145–165.
- Wiesner, M.G., Zheng, L., Wong, H.K., Wang, Y., Chen, W., 1996. Fluxes of particulate matter in the South China Sea. In: Ittekkot, V., Schäfer, P., Honjo, S., Depetris, P.J. (Eds.), *Particle Flux in the Ocean*. Wiley, New York, pp. 293–312.
- Winn, K., Zheng, L., Erlenkeuser, H., Stoffers, P., 1992. Oxygen/carbon isotopes and paleo-productivity in the South China Sea during the past 110,000 years. In: Jin, X., Kudrass, H.R., Pautot, G. (Eds.), *Marine Geology and Geophysics of the South China Sea*. China Ocean Press, Beijing, pp. 154–166.
- Zheng, L., 1987. A preliminary study on foraminifera in surface sediments of the central South China Sea (in Chinese, with English abstr.) *Donghai Mar. Sci.* 5 (1–2), 19–41.